Available online at www.sciencedirect.com
ScienceDirect
ELSEVIER
Dyes and Pigments 75 (2007) 225−245
DYES and PIGMENTS
www.elsevier.com/locate/dyepig

The photo-oxidation of reactive azobenzene dyes and an analysis of their reactivity for the azo and hydrazone tautomers using the semiempirical molecular orbital PM5 method

Toshio Hihara [a,*], Yasuyo Okada [b], Zenzo Morita [c]

[a] *Technical Center, DyStar Japan Ltd., Azuchi-machi 1-7-20, Chuo-ku, Osaka 541-0052, Japan*
[b] *School of Domestic Science, Otsuma Women's University, Sanban-cho, Chiyoda-ku 102-8357, Japan*
[c] *Tokyo University of Agriculture and Technology, Koganei, Tokyo 184-8588, Japan*

Received 24 November 2005; accepted 18 May 2006

Abstract

The photo-oxidative reaction of eight reactive azobenzene dyes with singlet oxygen ($^1O_2$) was examined by exposing the dyed cellulose films on immersion in an aerobic aqueous Rose Bengal solution, and the second-order rate constants, k_0, of the reaction were determined. The standard enthalpies of formation for these dyes in the gas phase and water, as calculated by the PM5 method, indicated that six of the dyes existed as azo tautomers in both the phases without exhibiting the azo−hydrazone tautomerism, and that the remaining two phenylazo dyes existed as hydrazone tautomers. The reaction sites and their reactivity for the corresponding tautomer on cellulose with $^1O_2$ were analyzed in accordance with frontier orbital theory. The positions were primarily the carbon atom of the coupling component at which the coupling reaction occurred for both of the tautomers. The reaction modes occurring between the azo dyes and $^1O_2$ were the ene and/or [2 + 2] cycloaddition reactions, and they occurred at the double bonds whose constituent atoms had larger Fukui electrophilic frontier densities, $f_r^{(E)}$. The reactivities of the azo dyes against $^1O_2$ were expressed by the sum of $f_r^{(E)}$ at the corresponding double bonds. The plots of log k_0 against the sum of $f_r^{(E)}$ for all the dyes examined gave a close mutual correlation. The sum of $f_r^{(E)}$ thus became a molecular descriptor of the reactivity of aromatics against $^1O_2$.

Keywords: Reactive dye; Azobenzene; Azo−hydrazone tautomerism; Singlet oxygen; Molecular orbital method; Electrophilic frontier density; Photo-oxidation; Ene reaction; [2 + 2] Cycloaddition

1. Introduction

The photo-oxidative fading of phenylazo- and naphthylazo-pyrazolinyl reactive dyes and monoazo dyes derived from γ- and J-acid was examined by exposing the dyed cellulose films on immersion in an aerobic aqueous Rose Bengal solution, and their reactivity toward singlet oxygen, $^1O_2$, was analyzed based on the results calculated using the semiempirical molecular orbital (MO) PM5 method [1,2]. In the processes, the dyes carried out the ene and [2 + 2] cycloaddition reactions with $^1O_2$. Between the second-order rate constants, k_0, of the reaction of the azo dyes with $^1O_2$ and the molecular descriptor of the reactivity based on the frontier orbital theory, a close relation was found to exist as a linear correlation between log k_0 and the sum of $f_r^{(E)}$ ($f_r^{(E)}$: electrophilic frontier electron density) for the double bonds to which $^1O_2$ attached. These results were consistent with the absorption spectra of the decomposed products.

Besides the ene and [2 + 2] cycloaddition reactions with $^1O_2$, which have been summarized in previous papers [1,2], the photochemical oxidation of aromatic compounds, such as aromatic amines, phenols and aryl ethers, has also been examined [3−7]. Unlike pyrazoline [1], naphthalene [2] and anthraquinone, benzene derivatives usually possess no double

---

* Corresponding author. Tel.: +81 6 6263 6681; fax: +81 6 6263 6697.
E-mail address: hihara.toshio@dystar.com (T. Hihara).

0143-7208/$ - see front matter © 2006 Elsevier Ltd. All rights reserved.
doi:10.1016/j.dyepig.2006.05.032

bonds in fixed positions, although several substituents of azobenzene dyes may fix them. Since the [4 + 2] cycloaddition of $^1O_2$ to aromatics has resulted in little decomposition but reversible adsorption, the decomposition of aromatic compounds, such as nucleic acids, has been reported to occur via the [2 + 2] cycloaddition of $^1O_2$ [8–11].

The azo–hydrazone tautomerism (AHT) of azobenzenes and phenylazopyrazolines in the gas phase and water was analyzed using the semiempirical MO method [12,13]. In previous papers [13,14], on the other hand, the present authors have discussed the reaction of azo and hydrazone tautomers (A&HTs) with $^1O_2$ and revealed that the A&HTs possess reactivities toward $^1O_2$ which are similar to each other, although recent detailed analyses have revealed different reactivity behaviors [1,2].

When the PM5 method was applied to the reactive dyes, all of the reactive groups were assumed to react with hydroxyl groups but not with cellulose, although the dyes on cellulose must bind with the hydroxyl groups of cellulose. The present authors took this assumption as a starting point, in order to discuss the AHT and the reactivity of reactive dyes in a cellulose–reactive dye system.

In the present paper, the photo-oxidation, or the reaction with $^1O_2$, of several yellow azobenzene dyes is examined by using dyed cellophane films; the positions of reaction and their corresponding reactivities for A&HTs are analyzed in terms of the frontier orbital theory; finally, the issue of whether or not the results of the analyses are consistent with the absorption spectra of the decomposed products bound to the cellulose is discussed. Thus, for dyes that exist as different tautomers in both the gas phase and water, the reactivity of both tautomers toward $^1O_2$ in the gas phase is analyzed based on the MO theory. For dyes which show no change in AHT in the two phases, the reactivity of the tautomers is examined.

2. Experimental

2.1. Yellow dyes used

Almost all the dyes used in this study were the same as those examined in a previous paper [12], and typical yellow azo dyes with other chemical structures were added. The chemical structures (unless otherwise stated, the structures of the azo tautomer are given), C.I. Generic Name, C.I. Constitution Number, and abbreviations (in parentheses) are shown below:

(1) C.I. Reactive Yellow 3, C.I. 13245, Procion Yellow HA (Yellow 3)

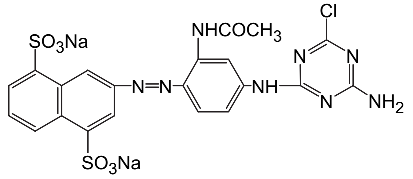

(2) An acetoaminophenylazo vinylsulfonyl (VS) dye, (Acetyl VS1)

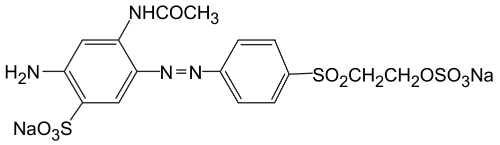

(3) A diaminophenylazo dye, (Diamino VS)

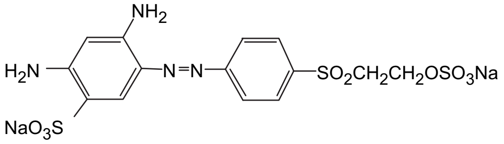

(4) An acetylaminoazo triazinyl VS dye, (Acetyl VS2)

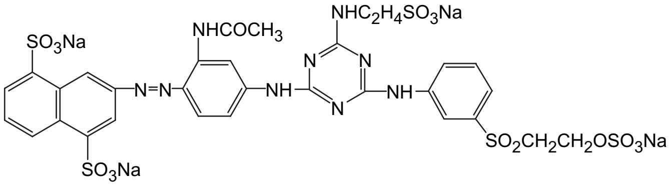

(5) A methylphenylazo triazinyl VS dye (Methyl VS)

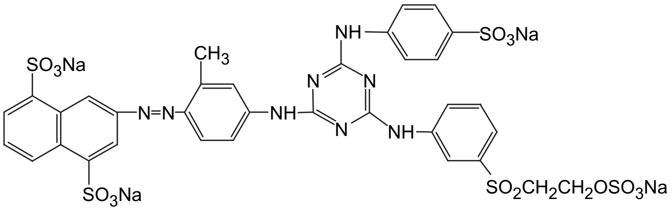

(6) An yellow azo dye with *m*-VS and monochlorotrazinyl (MCT) anchors (Ureido BF)

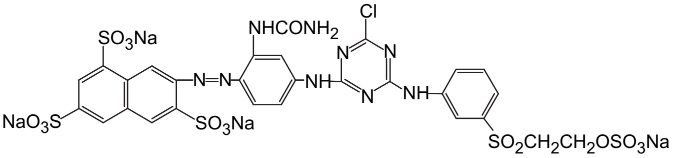

(7) An yellow azopyridone dye, hydrazone (Pyridone BF)

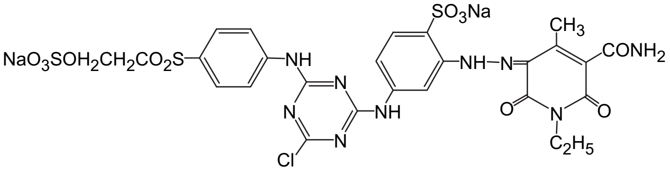

(8) An acetoamidomethylazo dye, hydrazone (Acetoacetyl VS)

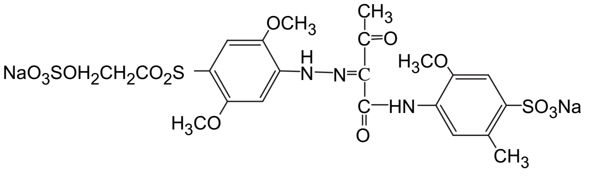

2.2. Dyeing of cellulose films and estimation of photo-oxidative fading by Rose Bengal

Cellophane films (Futamura Kagaku Kogyo, K.K. #300) were dyed with each dye through the alkali-shock method, in order to obtain an absorbance between 0.4 and 0.8 at λ_{max} [1,2,15,16]. By exposing the cellophane films dyed with reactive dyes to a carbon arc on immersion in an aerated aqueous Rose Bengal solution, the relative fading of the individual dyes could be estimated by the same method as before. It has been confirmed recently that RB generates only $^1O_2$ and that the formation of superoxide is a very inefficient process [17,18].

2.3. MO calculations

The MO calculations were done on CAChe MOPAC 2002 (Windows Version 6.1.10) (Fujitsu, Ltd.) as in the case of previous papers [1,2]. For the A&HTs of the eight yellow dyes (as well as the azo–keto tautomers (A/KT) of Acetoacetyl VS and the azo–enol tautomers (A/ET) of Pyridone BF) in the gas phase and water, structure optimization was performed in order to obtain their molecular parameters, such as the standard heat of formation (kcal/mol), the electron density at each atom in the HOMO, the electrophilic frontier density, the dipole moment (D), and the HOMO and LUMO energies (eV), using the PM5 method.

3. Results and discussion

3.1. Photo-oxidative fading of yellow reactive dyes or the ease with which the dye is photo-oxidized by Rose Bengal

The photosensitized oxidative fading of each dye on cellulose film was plotted as the relative fading profile for each dye against the time of exposure, as illustrated in Fig. 1. Referring to the rates of fading for pyrazolinylazo dyes estimated in a previous study [1], the order of the rate of fading for fifteen (including Pyr-Yellow) yellow azo dyes was as follows:

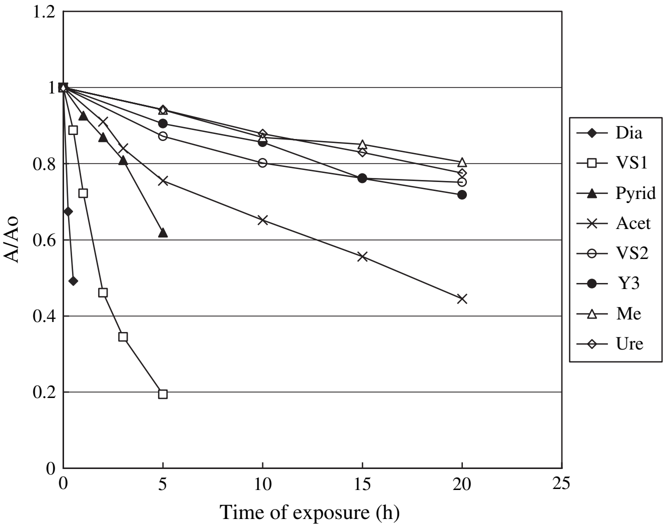

Fig. 1. Relative rates of photosensitive fading of azobenzene dyes on cellulose with Rose Bengal on exposure to carbon arc through Toshiba Y-51 filter.

$$\begin{aligned}\text{Pyr}-\text{Yellow} \gg \text{Diamino VS} > \text{Yellow 14} > \text{Yellow 2}\\ > \text{Yellow 17} > \text{Acetyl VS1} \gg \text{Yellow 13}\\ > \text{Pyridone BF} > \text{Carbopyr}-\text{Yellow}\\ > \text{Naphpyr}-\text{Yellow} > \text{Acetoacetyl VS}\\ > \text{Acetyl VS2} > \text{Yellow 3} > \text{Methyl VS}\\ \approx \text{Ureido BF}. \qquad (1)\end{aligned}$$

Pyr-Yellow was much more easily photo-oxidized than the other azo dyes examined [15,16], while some pyrazolinylazo dyes were harder to photo-oxidize than the azobenzene dyes.

The order of the rate of fading for the arylazobenzene dyes was as follows:

$$\begin{aligned}\text{Diamino VS} \gg \text{Acetyl VS1} \gg \text{Pyridone BF}\\ > \text{Acetoacetyl VS} > \text{Acetyl VS2} > \text{Yellow 3}\\ > \text{Methyl VS} \approx \text{Ureido BF}. \qquad (2)\end{aligned}$$

And the order for the pyrazolinylazo dyes was [1]:

$$\begin{aligned}\text{Pyr}-\text{Yellow} > \text{Yellow 14} > \text{Yellow 2} > \text{Yellow 17}\\ > \text{Yellow 13} > \text{Carbopyr}-\text{Yellow}\\ > \text{Naphpyr}-\text{Yellow}. \qquad (3)\end{aligned}$$

The k_0 values (dm^3/mol/s) for the reaction between the dyes and $^1O_2$ were estimated from the initial slope of fading illustrated in Fig. 1, using the k_0 value of Pyr-Yellow as the reference [15] together with the values of the pyrazolinylazo dyes [1]. The results are listed in Table 1. Half of the azobenzene dyes generally used have smaller k_0 values than the typical red azo dyes produced from H-acid, in contrast to the pyrazolinylazo dyes [16].

3.2. Azo–hydrazone tautomerism on cellulose

The AHT of hydroxyazo and aminoazo dyes depends on the solvation or the environment in which the dyes exist. In order to analyze the AHT, the standard enthalpies, Δ_fH^0(gas) and $\Delta_fH^0(H_2O)$ (kcal/mol), of formation for dyes in the gas phase and in water were estimated using the PM5 method, as listed in Tables 2 and 3, and as described in previous papers [1,2,12–14]. The tautomers, which are supposed to predominate according to the values of Δ_fH^0(gas) and $\Delta_fH^0(H_2O)$, are summarized in Table 4.

The AHTs coincided with the results described in a previous paper [12], even though some new dyes were added in the present study. The absolute values of Δ_fH^0(gas) and $\Delta_fH^0(H_2O)$ for the individual dyes were considerably different depending upon the Hamiltonian (AM1, PM3 and PM5) and,

Table 1
Values of the rate constant, k_0 (dm^3/mol/s), of the second-order reaction with $^1O_2$ estimated from the initial slope of relative fading, A/A_0, for yellow reactive dyes on cellulose immersed in aerated Rose Bengal (3.3×10^{-5} M + 0.5 M Na_2SO_4) solution on exposure to carbon arc through a Toshiba filter Y-51, and their supposed mode of reaction with singlet molecular oxygen

	Yellow dyes	k_0	Absorption spectra of the decomposition product on cellulose
1	Yellow 3[a]	0.048	$\lambda_{max} = 210$ nm (with small shoulders)
2	Diamino VS	3.31	Nearly similar to each other
3	Acetyl VS1	0.71	Similar to Yellow 13 [1]
4	Acetyl VS2	0.056	Low double peaks,
5	Ureido BF	0.029	nearly similar to
6	Methyl VS	0.030	each other
7	Pyridone	0.187	Similar to Yellow 2 [1]
8	Acetoacetyl	0.104	Same as Yellow 17 [1]

[a] C.I. Reactive Generic Name.

to a much lesser extent, upon the version of PM5 employed, and the differences in the absolute values of $\Delta_f H^0$(gas) and $\Delta_f H^0(H_2O)$ for the individual dyes varied with the chemical structures calculated. The MO calculations, however, resulted in almost the same estimation of AHT.

Unfortunately, however, there is no procedure to clarify the solvation effects of dyes in solid polymer; they can be described only for dyes in pure liquid. In the present study, the photo-oxidative fading of dyes by Rose Bengal was examined under the wet condition, or in water-swollen cellulose. The extent of solvation for dyes in cellulose was regarded to lie between the extent of solvation in the gas phase and that in water [1,2]. Therefore, in the present study it was considered that the reactivity of the tautomers in cellulose could be approximated to that of the corresponding tautomers in the gas phase. The fact that the λ_{max}s of the azo dyes on cellophane are shifted from those in organic solvents and far from in water may be an indirect evidence of the approximation.

In previous papers [1,2] and in the present study, the AHT estimated by the PM5 method was indirectly demonstrated to be valid. The reactivity derived from the MO theory on the basis of AHT showed a good correlation with the corresponding experimental results, as explained below.

3.3. Photodecomposed products of yellow azo dyes bound with cellulose

In previous papers [1,2] and a in series of other papers [19–23], the photodecomposition of reactive dyes on cellulose was analyzed by determining the absorption spectra of the decomposed products. The patterns of the absorption spectra of the decomposed products bound with cellulose were classified into several groups of reactive anchors, as summarized in Table 1. The same spectral pattern as the previous ones was also referred [1,2]. The reaction schemes with $^1O_2$ are discussed in Section 3.5.

Table 2
Enthalpy of formation, $\Delta_f H^0$(gas) and $\Delta_f H^0(H_2O)$ (kcal/mol), dipole moment, μ (D), HOMO and LUMO energies (eV), for azo and hydrazone tautomers of Yellow 3, Diamino VS, Acetyl VS1 and Acetyl VS2 in the gas phase, and electrophilic frontier density, $f_r^{(E)}$, for the most probable tautomer, estimated by PM5 method (cf. Tables 5 and 6)

Dye	Yellow 3 (Y3)		Diamino VS (Dia)		Acetyl VS1 (VS1)		Acetyl VS2 (VS2)	
M.W.	574.542		400.424		442.461		865.878	
	AT	HT	AT	HT	AT	HT	AT	HT
$\Delta_f H^0$(gas)	−173.377	−156.297	−152.512	−141.224	−199.795	−182.980	−348.430	−327.468
μ	4.397	5.096	4.598	5.033	4.199	3.049	3.103	2.319
E_{HOMO}	−9.124	−8.992	−9.180	−9.203	−9.412	−9.468	−9.221	−9.007
E_{LUMO}	−2.225	−1.982	−1.685	−2.144	−1.786	−2.478	−2.258	−2.187
$\Delta_f H^0(H_2O)$	−233.305	−215.037	−198.620	−186.098	−247.139	−232.316	−429.142	−412.157
$f_r^{(E)}$ (position) for the most probable tautomer	AT		AT		AT		AT	
	0.284 (C13)		0.383 (C1)		0.374 (C1)		0.213 (C13)	
	0.125 (C14)		0.067 (C6)		0.098 (C6)		0.062 (C14)	
	0.143 (C16)		0.252 (C3)		0.267 (C3)		0.114 (C15)	
	0.205 (C17)		0.045 (C4)		0.058 (C4)		0.166 (C16)	
	0.046 (C1)		0.224 (C5)		0.173 (C5)		0.107 (C17)	
	0.044 (C10)		0.191 (N8)		0.064 (C14)		0.069 (C18)	
			0.053 (N7)		0.059 (C9)		0.039 (N11)	
	0.042 (C18)		0.068 (C10)		0.057 (C10)		0.066 (N12)	
	0.131 (N11)		0.058 (C9)					
	0.045 (N12)		0.062 (C14)		0.201 (N8)		0.037 (C1)	
	0.103 (C15)				0.077 (N7)		0.011 (C10)	
	0.035 (C4)		0.031 (C2)					
	0.016 (C9)							

$f_r^{(E)}$ (position): electrophilic frontier density at the corresponding atomic position.

Table 3
Enthalpy of formation, Δ_fH^0(gas) and $\Delta_fH^0(H_2O)$ (kcal/mol), dipole moment, μ (D), HOMO and LUMO energies (eV), for azo and hydrazone tautomers of yellow azo dyes in the gas phase, and electrophilic frontier density, $f_r^{(E)}$, for the most probable tautomer, estimated by PM5 method (cf. Tables 5 and 6)

Dye	Ureido BF (Ure)		Acetoacetyl VS (Acet)		Pyridone BF (Pyr)			Methyl VS (Me)
M.W.	839.797		573.589		689.674			870.894
	AT	HT	A/KT[a]	HT	AT	A/ET[b]	HT	AT
Δ_fH^0(gas)	−389.895	−377.843	−350.819	−350.194	−264.078	267.764	−275.061	−273.804
μ	11.763	9.902	7.448	6.065	10.997	9.921	7.115	4.777
E_{HOMO}	−9.259	−9.553	−9.573	−9.708	−9.130	−9.061	−9.934	−9.313
E_{LUMO}	−2.466	−2.294	−1.698	−1.693	−1.875	−1.851	−2.086	−2.199
$\Delta_fH^0(H_2O)$	−479.523	−472.956	−399.003	−402.754	−341.504	−343.645	−343.637	−360.249
$f_r^{(E)}$ (position) for the most probable tautomer	AT		A/KT	HT	A/ET	HT		AT
	0.289 (C13)		0.179 (C6)	0.239 (C6)	0.372 (C1)	0.092 (C1)		0.055 (C18)
	0.105 (C14)		0.080 (C1)	0.066 (C1)	0.059 (C2)	0.036 (N7)		0.214 (C13)
	0.114 (C16)		0.179 (C9)	0.129 (C4)	0.295 (C3)	0.103 (C3)		0.075 (C14)
	0.215 (C17)		0.053 (C10)	0.056 (C5)	0.119 (N7)	0.028 (C2)		0.091 (C15)
			0.059 (N8)	0.070 (C2)	0.219 (N8)	0.042 (C9)		0.140 (C16)
	0.096 (C15)		0.063 (N7)	0.093 (C3)	0.090 (C10)	0.132 (C10)		0.094 (C17)
	0.128 (N11)		0.077 (C4)		0.057 (C9)	0.129 (C12)		0.063 (C1)
	0.031 (N12)		0.090 (C5)	0.073 (C9)	0.070 (C14)	0.028 (C13)		0.052 (C10)
			0.060 (C2)	0.026 (N8)	0.095 (C12)	0.140 (C14)		
			0.121 (C3)		0.026 (C13)			0.136 (N11)
						0.030 (N5)		0.082 (N12)
					0.020 (C11)	0.002 (C6)		0.021 (C9)
					0.022 (N5)			0.041 (C4)
					0.014 (C6)			

$f_r^{(E)}$ (position): electrophilic frontier density at the corresponding atomic position.

[a] Azo/keto tautomer = A/KT.

[b] Azo/enol tautomer = A/ET.

Group A (two azobenzene dyes with a *p*-vinylsulfonylphenyl anchor in the diazo component). Acetyl VS1 and Diamino VS each possessing a 4-(2-hydroxyethylsulfonyl)-phenyl group as the anchor system constitute this group. The decomposed products of the two dyes gave nearly the same absorption spectra (Fig. 2). The coupling components had no effect on the spectra, but only on the rates of photo-oxidation.

Group B (azo dyes with a 2,5-dimethoxy-4-vinylsulfonylphenyl anchor in the diazo component). Acetoacetyl VS belongs to this group, like Yellow 17 [1]. The two dyes gave spectra similar in pattern but different in the detailed structure (Fig. 2).

Group C (azo dyes with an MCT or a heterobifunctional VS/MCT anchor). Yellow 3, Ureido BF and Pyridone BF belong to this group. The first two dyes showed smaller rates of fading than the last dye. The patterns of the absorption spectra for Acetyl VS2, Ureido BF and Methyl VS (Fig. 3) had low double peaks, while that for Pyridone had big double peaks (Fig. 4) and that for Yellow 3 had a single peak with small shoulders (Fig. 2). The peak on the shorter wavelength side may be attributed to the triazine group, and that on the longer wavelength side to the phenyl group. Although the differences between the detailed structures of the first three dyes were not clear based on the absorption spectra of the decomposed products, the patterns of the spectra were clearly different from each other (Figs. 3 and 4).

Group D (azo dyes with a VS anchor attached to a triazinyl ring in the coupling component). Acetyl VS2 and Methyl VS belong to this group. The absorption spectra of the decomposed products for these dyes as well as for Ureido BF were similar in pattern (Fig. 3).

As discussed in previous papers [1,2], $^1O_2$ was added to the double bonds, and most of the oxygen molecules attached to bridge groups such as azo and imino groups to generate 1,2-dioxetanes via [2 + 2] addition or hydroperoxides via the ene reaction. The intermediates generated were thermally and/or photochemically decomposed further, resulting in the corresponding ring opening followed by the C−N bond scission. Thus, the aromatic residues with anchor groups bound to the cellulose remained, although they could also have been a mixture of decomposed products from the corresponding dye.

3.4. Reactivity of yellow azo dyes in terms of frontier electron density

Chemical reactions between $^1O_2$ and organic compounds such as hydroxylazo dyes and heterocycles have been revealed to as being mainly two different reaction modes providing (1) dioxetanes or carbonyl fragments via [2 + 2] addition (dioxetane reaction), and (2) allylic hydroperoxides via 1,3-addition (ene reaction) [8–11, 24–29]. In each reaction mode, several reaction mechanisms are known to operate, although the preference for one mechanism over another is dependent upon the experimental conditions. Using the same procedure as described in previous papers [1,2], a comparison of the reactivities of the eight azobenzene dyes was done in terms of frontier electron density.

Table 4
Predominant tautomers in the gas and water phases estimated by $\Delta_f H^0$(gas) and $\Delta_f H^0$(water) using PM5 method, their probable primary mode of reaction for the tautomer with singlet oxygen (cf. Tables 2, 3, 5 and 6), and the atomic position of their reactions

Yellow dyes	Predominant tautomer (phase)[a]	Probable primary mode of reaction (position)		
		Ene (commonly)	[2 + 2] Addition (commonly)	[2 + 2] Addition (uniquely probable)
Diamino VS Acetyl VS1	AT(g&w)	C3=C4, C5=C4; H(N16)	C1=C6, C3=C4, C4=C5, C9=C10, C9=C14	N7=N8
Yellow 3 Acetyl VS2 Ureido BF	AT(g&w)	C13=C14; H(N21)	C13=C14, C16=C17	C1=C10 C15=C16, C17=C18, N11=N12
Methyl VS		C13=C14;H(Me)		C1=C10, C15=C16, C13=C18
Acetoacetyl VS	A/KT(g)/HT(g) → HT(w)	A/KT: C9=N8;H(N7) HT: C1=C6	A/KT: C1=C6, C2=C3, C4=C5; N7=N8; C9=C10 HT: C1=C6, C2=C3, C4=C5	
Pyridone BF	HT(g) → A/ET(w)/HT(w)	HT: C1=N7; H(N8) A/ET: C1=C2; H(Me)	HT: C2=C3; C1=N7; C10=C9, C12=C13, C13=C14 A/ET: C1=C2, C2=C3; N7=N8; C9=C10, C9=C14, C12=C13	

[a] g = Gas, w = water.

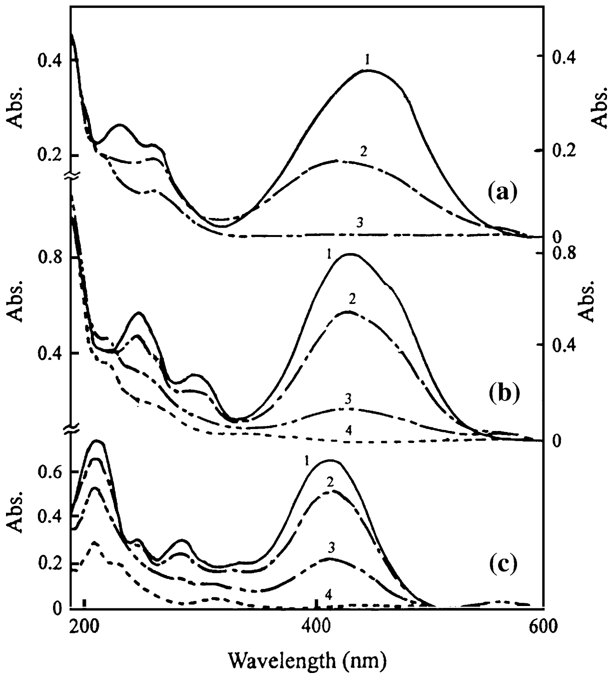

Fig. 2. Absorption spectra of the original dye (1) and of the decomposed products on cellophane film immersed in Rose Bengal solution after exposure to carbon arc through a Toshiba Y-51 filter for following times of exposure: (a) for Diamino VS and the exposure for 30 min (2) and 5 h (3) (completely decomposed product), (b) for Acetyl VS1 and the exposure for 1 h (2), 5 h (3) and the calculated spectrum (4) of the decomposed products reducing with that of the original one from the spectrum (3), and (c) for Acetoacetyl and the exposure for 5 h (2), 25 h (3) and the calculated spectrum (4) of the decomposed products reducing with that of the original one from the spectrum (3).

Fukui et al. [30–33] have introduced a factor called the frontier electron density, $f_r^{(E)}$, for the electrophilic reaction; it is the weighted sum of the squares of the coefficients of the LCAO MO. Fukui's original expression can be rendered as follows:

$$f_r^{(E)} = \frac{\sum_{j=1}^{N} \nu_j \left(C_r^j\right)^2 \exp\left\{-\lambda\left(E_{\mathrm{HOMO}} - E_j\right)\right\}}{\sum_{j=1}^{N} \nu_j \exp\left\{-\lambda\left(E_{\mathrm{HOMO}} - E_j\right)\right\}}. \quad (4)$$

In this equation, N is the total number of orbitals, ν_j is the number of electrons in the jth orbital and is usually 0, 1, or 2, C_r^j is the coefficient of the jth LCAO MO at the rth atomic position, E_j is the energy of the jth orbital, and λ is a scale factor that is usually set to 3.0 in these calculations [34].

3.5. Reaction modes of azobenzene dyes

The electrophilic reactivity of the double bonds toward $^1O_2$ may be described by the sum $S_{m,n}^{(E)}$ of the $f_r^{(E)}$ defined by Eq. (4) at the two adjacent atomic positions, as follows [1,2]:

$$S_{m,n}^{(E)} = \sum_{m,n} \left\{ f_m^{(E)} + f_n^{(E)} \right\}, \quad (5)$$

where m and n denote the atomic positions of the corresponding double bonds; when these positions overlap, the position is

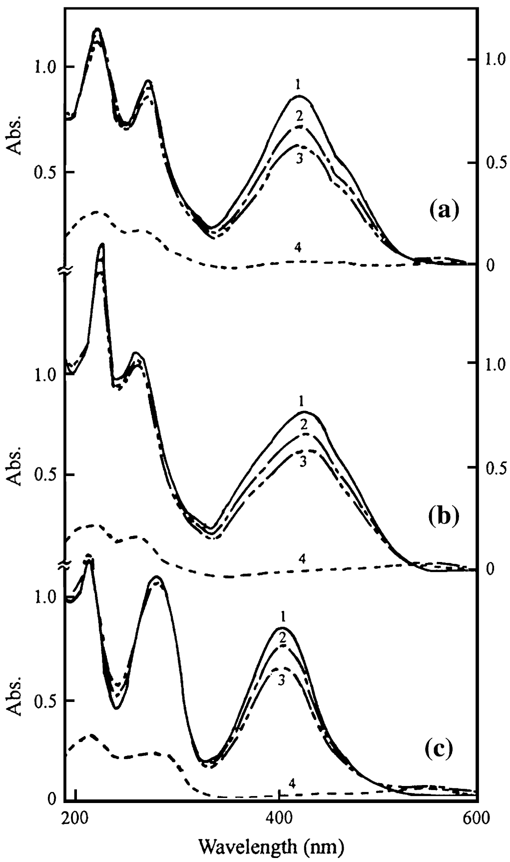

Fig. 3. Absorption spectra of the original dye (1) and of the decomposed products on cellophane film immersed in Rose Bengal solution after exposure to carbon arc through a Toshiba Y-51 filter for (a) Acetyl VS2, (b) Ureido BF (2) and (c) Methyl VS for following times of exposure: for 10 h (2) and 20 h (3), and the calculated spectrum (4) of the decomposed products reducing with that of original one from the spectrum (3).

counted only once. The double bonds with a larger value of $\left(f_m^{(E)} + f_n^{(E)}\right)$ are taken into consideration one by one.

According to the previous procedure for the analysis of the reactivity [1,2] of the ene and the [2 + 2] cycloaddition reactions for AT or HT with $^1O_2$, the $S_{m,n}^{(E)}$ values for the two atoms of the double bond, to which $^1O_2$ may attach, were plotted against log k_0, as shown in Fig. 5. According to the frontier orbital theory, the position of reaction with $^1O_2$ may be taken as the atomic position with the largest electron density, d_{HOMO}, of HOMO, and the reactivity may be taken as being proportional to the $S_{m,n}^{(E)}$ values, although whether a certain reaction mode will be launched or not, and whether the same reaction will occur at the position of the next largest $S_{m,n}^{(E)}$ value (one after the other) or not, must be determined based on the experimental results. The values of d_{HOMO} for the eight dyes, as calculated by the PM5 method, are listed in Tables 5 and 6. The possible reaction modes and their primary positions are summarized in Table 4. The positions on the ordinate (log k_0) were determined or fixed by the experiments, while those of the abscissa were determined so as to find a general correlation between log k_0 and the $S_{m,n}^{(E)}$ values. The course of analysis for the individual dyes is explained next.

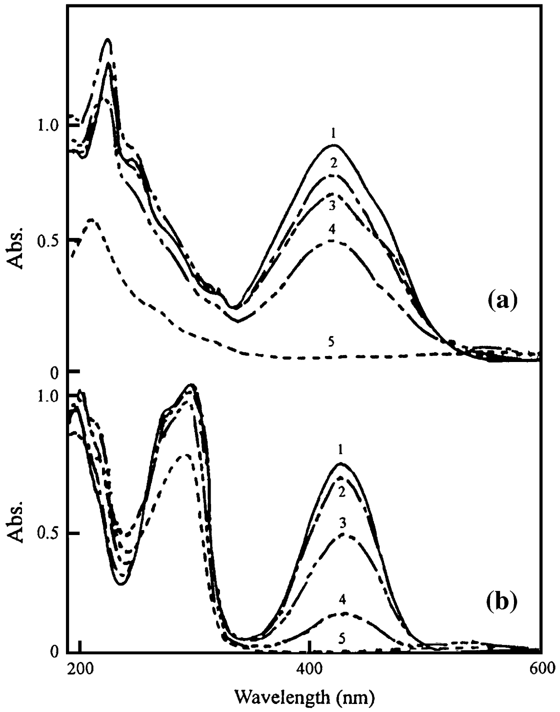

Fig. 4. Absorption spectra of the original dye (1) and of the decomposed products on cellophane film immersed in Rose Bengal solution after exposure to carbon arc through a Toshiba Y-51 filter for following times of exposure: (a) for Yellow 3 and the exposure for 10 h (2), 20 h (3), 40 h (4) and the calculated spectrum (5) of the decomposed products reducing that of original one from the spectrum (4) and (b) for Pyridone and the exposure for 1 h (2), 5 h (3), 15 h (4) and the calculated spectrum (5) of the decomposed products reducing with that of original one from the spectrum (4).

3.5.1. Reaction modes of ATs of 2-arylamino-4-aminophenylazobenzene dyes with a VS anchor in diazo component (Group A)

Diamino VS and Acetyl VS1 belong to this group. Except for the acetyl substituent on the *o*-amino group, the

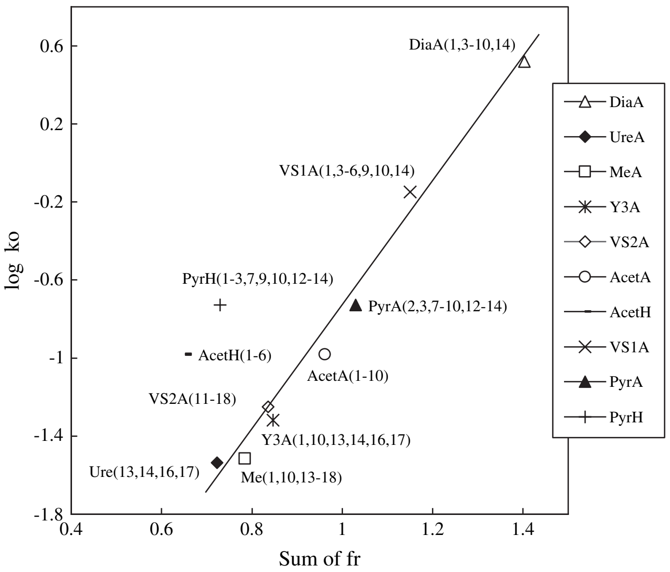

Fig. 5. Relationship between log k_0 and the sum of $f_r^{(E)}$ for a series of azobenezene dyes.

Table 5
Electron density, d_{HOMO}, of HOMO at each atomic position for azo, azo/enol and hydrazone tautomers of Diamino VS, Acetyl VS1, Pyridone VS, Acetoacetyl VS in the gas phase, calculated using PM5 method

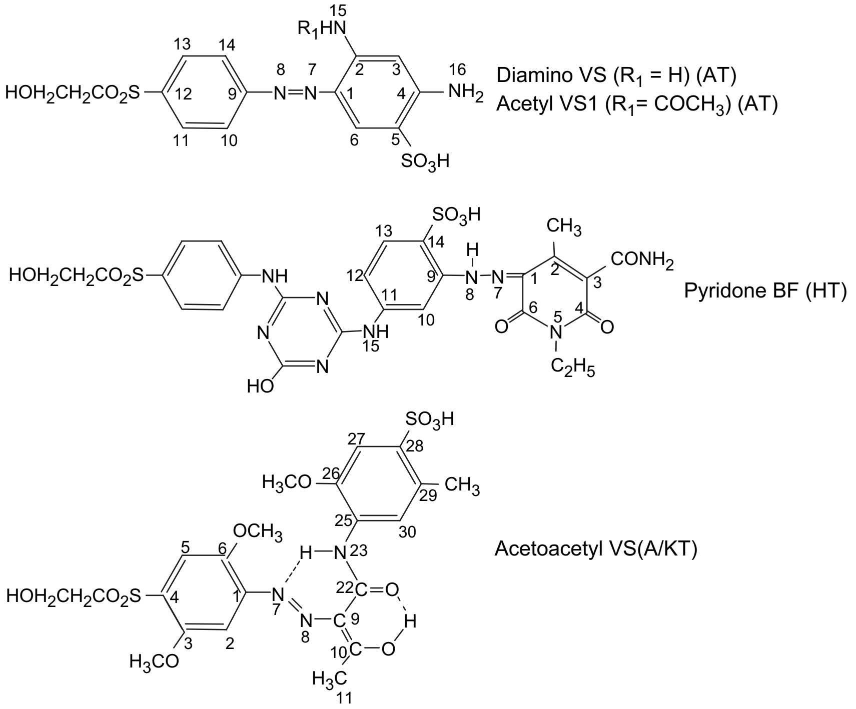

	Diamino VS		Acetyl VS1			Pyridone BF			Acetoacetyl VS	
	AT	HT	AT	HT		A/ET	HT		A/KT	HT
C1	0.280	0.188	0.245	0.187	C1	0.244	0.100	C1	0.068	0.065
C2	0.008	0.000	0.000	0.001	C2	0.040	0.019	C2	0.036	0.018
C3	0.027	0.045	0.143	0.082	C3	0.191	0.086	C3	0.129	0.087
C4	0.027	0.005	0.040	0.008	C4	0.006	0.000	C4	0.083	0.129
C5	0.150	0.100	0.106	0.128	N5	0.001	0.000	C5	0.088	0.041
C6	0.043	0.005	0.065	0.009	C6	0.008	0.000	C6	0.201	0.246
N7	0.011	0.020	0.006	0.017	N7	0.058	0.031	N7	0.018	0.127
N8	0.115	0.268	0.091	0.207	N8	0.125	0.214	N8	0.017	0.016
C9	0.034	0.030	0.018	0.019	C9	0.029	0.047	C9	0.031	0.055
C10	0.038	0.068	0.020	0.041	C10	0.040	0.012	C10	0.011	0.001
C11	0.002	0.001	0.001	0.001	C11	0.000	0.019	C11	0.000	0.000
C12	0.056	0.090	0.028	0.050	C12	0.052	0.161	C22	0.002	0.000
C13	0.001	0.001	0.001	0.001	C13	0.012	0.014	N23	0.009	0.002
C14	0.037	0.063	0.021	0.037	C14	0.027	0.133	C25	0.001	0.000
N15	0.041	0.102	0.000	0.162	N15	0.000	0.061	C26	0.005	0.002
N16	0.114	0.000	0.200	0.001				C27	0.000	0.000
								C28	0.004	0.001
								C29	0.000	0.000
								C30	0.000	0.000

other parts of structure are the same for these two dyes (cf. Table 5). Table 1 shows that the rates of photosensitized oxidative fading are: Diamino VS ≫ Acetyl VS1. The electrons in HOMO are concentrated within the coupling component, as listed in Table 5. This may indicate that these dyes have very high reactivities against $^1O_2$ in the coupling component, and that the reactions may occur there. As shown in Table 5, the electron densities of HOMO (d_{HOMO}) for the ATs of the two dyes are similar, although the values of d_{HOMO} for Diamino VS are almost always higher than those for Acetyl VS1 at the probable reaction sites. As explained above and as reported previously [1,2], the reaction against $^1O_2$ may well be described by $f_r^{(E)}$, whose values at the atomic positions of the double bonds in the coupling component are listed in Table 2. These values could suggest that the reactions occur at the double bonds of C1=C6, C3=C4, C4=C5, C9=C10, C9=C14 and N7=N8. The differences in the reaction mode between the two dyes are discussed next.

3.5.1.1. ATs of Diamino VS. Based on the $S_{m,n}^{(E)}$ values for the corresponding double bonds (cf. Table 2), the possible reaction modes for the ATs of Diamino VS were determined. The values of $\Delta_f H^0$(gas) for the corresponding reaction

Table 6
Electron density, d_{HOMO}, of HOMO at each atomic position for the azo and hydrazone tautomers of Yellow 3, Acetyl VS2, Ureido BF, and Methyl VS in the gas phase, calculated using PM5 method

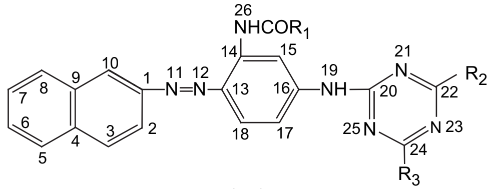

(AT)

	Yellow 3		Acetyl VS2		Ureido BF		Methyl VS
	AT	HT	AT	HT	AT	HT	AT
C1	0.021	0.049	0.021	0.039	0.006	0.007	0.040
C2	0.008	0.028	0.003	0.027	0.003	0.001	0.015
C3	0.004	0.008	0.001	0.009	0.002	0.001	0.006
C4	0.013	0.047	0.001	0.038	0.009	0.005	0.026
C5	0.000	0.002	0.000	0.001	0.000	0.000	0.001
C6	0.008	0.033	0.001	0.027	0.006	0.004	0.021
C7	0.000	0.005	0.000	0.003	0.000	0.000	0.003
C8	0.005	0.015	0.000	0.013	0.004	0.003	0.008
C9	0.003	0.011	0.001	0.007	0.000	0.000	0.009
C10	0.026	0.081	0.004	0.068	0.027	0.018	0.037
N11	0.071	0.250	0.025	0.225	0.086	0.073	0.089
N12	0.007	0.040	0.049	0.036	0.008	0.053	0.037
C13	0.195	0.129	0.180	0.121	0.220	0.034	0.183
C14	0.071	0.000	0.026	0.000	0.068	0.000	0.041
C15	0.009	0.057	0.074	0.080	0.005	0.230	0.047
C16	0.095	0.008	0.144	0.010	0.081	0.075	0.123
C17	0.131	0.086	0.071	0.092	0.156	0.077	0.060
C18	0.000	0.037	0.040	0.042	0.000	0.095	0.030
N19	0.131	0.003	0.214	0.007	0.115	0.101	0.131
C20	0.007	0.000	0.013	0.000	0.005	0.000	0.009
C21	0.023	0.001	0.040	0.002	0.021	0.025	0.025
C22	0.000	0.000	0.000	0.000	0.000	0.000	0.000
C23	0.019	0.000	0.035	0.001	0.017	0.020	0.019
C24	0.000	0.000	0.000	0.000	0.000	0.000	0.000
C25	0.027	0.001	0.038	0.002	0.023	0.023	0.024
N26	0.081	0.083	0.001	0.110	0.105	0.121	(26 = Me)

Yellow 3 ($R_1 = CH_3$; $R_2 = OH$; $R_3 = NH_2$; 3,8-disulfonic acid).
Acetyl VS2 ($R_1 = CH_3$; $R_2 = NHC_2H_4SO_3H$; $R_3 =$ *m*-(β-hydroxyethylsulfonyl)anilino; 3,8-disulfonic acid).
Ureido BF ($R_1 = NH_2$; $R_2 = OH$; $R_3 =$ *m*-(β-hydroxyethylsulfonyl)anilino; 2,6,8-trisulfonic acid).
Methyl VS ($R_2 =$ *p*-sulfoanilino; $R_3 =$ *m*-(β-hydroxyethylsulfonyl)anilino; 3,8-disulfonic acid; $26 = CH_3$).

intermediates of the possible modes in PM5 geometry and in PM5 transition-state geometry (TSG), as well as those for their products, were calculated. The results are listed in Tables 7–9. The values of $\Delta_f H^0$(gas) for the intermediates in PM5 geometry and in PM5 TSG were almost the same for each mode. Since the $\Delta_f H^0$(gas) values for the intermediates in TSG did not always correlate with the corresponding values of $S_{m,n}^{(E)}$, the reactivity of each double bond was estimated based on the values of $\Delta_f H^0$(gas) for the products, as follows:

$$\begin{aligned} \mathrm{ene(C3{=}C4;H(N16))} &> \mathrm{[2+2]addition(C3{=}C4)} \\ &> \mathrm{[2+2]addition(C1{=}C6)} \\ &> \mathrm{[2+2]addition(C3{=}C2)} \\ &> \mathrm{ene(C1{=}C2;H(N15))} \\ &\gg \mathrm{[2+2]addition(C10{=}C9)} \\ &= \mathrm{[2+2]addition(C9{=}C14)} \\ &> \mathrm{[2+2]addition(C1{=}C2)} \\ &> \mathrm{ene(C5{=}C4;H(N16))} \\ &\gg \mathrm{[2+2]addition(C4{=}C5)} \\ &\gg \mathrm{[2+2]addition(N7{=}N8)}. \end{aligned} \qquad (6)$$

Of the eleven modes given above, it should be discussed whether three of them, ene (C3=C2; H(N15)) and [2 + 2] addition (C1=C2 and C2=C3), contribute to the reactivity or not, because d_{HOMO} (0.015) and $f_r^{(E)}$ (0.025) at C2 may indicate the lower limit of reactivity [1]. These modes may not be unequivocally determined, although the neighboring sites of C1 and C3 contribute to the reactivity due to the large $f_r^{(E)}$ values at the neighboring sites, C6 and C4. (As mentioned below, whether the contribution of C2 is to be excluded or not depends on which of two $S_{m,n}^{(E)}$ values is chosen for examination together with the values for all the dyes used.) On the other hand, [2 + 2] addition (C10=C9) may be regarded as being the same as [2 + 2] addition (C9=C14), although these double bonds may show a smaller reactivity than the other bonds. As in the case of a previous study [1], the double bond of N7=N8 may possess a high reactivity against $^1O_2$, irrespective of the high activation energies. The inequality (6) and the $S_{m,n}^{(E)}$ values may imply that the atomic positions of C1 and C3–C6 have high reactivities against $^1O_2$.

Thus, the inequality (6) may be not consistent with the order based on the $S_{m,n}^{(E)}$ values listed in Table 3. If only the possible double bonds are mentioned, there are no differences between the values of $\Delta_f H^0$(gas) of the intermediates for any of the reaction modes, except for the bond of N7=N8.

These estimations may be confirmed by the spectral analysis of the exposed sample or the absorption spectra of the decomposed products bound with cellulose, which are illustrated in Fig. 2a. Although not completely identical, Acetyl VS1 gave the same absorption spectra of the decomposed products (cf. Section 3.5.1.2 and Fig. 2b). This fact may demonstrate that the present analyses are correct. In the beginning, what products each reaction mode yielded was analyzed. Of the eleven reaction modes, two, ene (C5=C4; H(N16)) and [2 + 2] cycloaddition (C5=C4), are illustrated in Scheme 1A and B, respectively. Ene (C1=C2; H(N15)) and [2 + 2] addition (C1=C2) correspond to ene (C1=C2; H(N20)) and [2 + 2] addition (C1=C2) for Pyr-Yellow in Scheme 1A and B from a previous report [1], although the pyrazoline ring must be read as a benzene ring. Since the other modes may be interpreted in analogy to these schemes, not all of the schemes are explicated. (For example, ene (C3=C4; H(N16) generates a 3-hydroperoxide, which may form the corresponding phenol as the main product via thermal dediazotization.) These schemes may imply the formation of a common product, 2-hydroxyethylsulfonylphenol, while phenylene–quinone–iminoquinone derivatives are formed as a by-product at different positions, although many other reaction modes

Table 7

Heat of formation, $\Delta_f H^0$(gas) (kcal/mol), of intermediate and products in the ene and [2 + 2] cycloaddition reactions at the double bonds of (C1═C2), (C3═C2), (C3═C4) and (C5═C4) for AT of pyrazolinylazo dyes with singlet oxygen

	Tautomer	M.W.	$\Delta_f H^0$(gas) of intermediate at TSG	$\Delta_f H^0$(gas) of intermediate	$\Delta_f H^0$(gas) of hydroperoxide	$\Delta_f H^0$(gas) of intermediate at TSG	$\Delta_f H^0$(gas) of intermediate	$\Delta_f H^0$(gas) of addition product
Mode (position)			Ene (C1═C2; H(N15))			[2 + 2] Addition (C1═C2)		
Acetyl VS1	AT	474.460	−176.364	−176.311	−199.216	−176.391	−176.360	−193.409
Diamino VS	AT	432.422	−136.169	−136.057	−157.445	−135.771	−135.769	−149.450
Mode (position)			Ene (C1═C2; H(Me))			[2 + 2] Addition (C1═C2)		
Pyridone BF	A/ET	721.672	−251.178	−251.178	−284.947	−249.863	−249.861	−272.045
Mode (position)			Ene (C1═N7; H(N8))			[2 + 2] Addition (C1═N7)		
Acetyl VS1	HT	474.460	−159.423	−159.421	−196.920[a]	−159.459	−159.316	−159.896[a]
Pyridone BF	HT	721.672	−255.187	−255.180	−299.579	−255.220	−255.212	−262.252
Mode (position)			Ene (C5═C4; H(N16))			[2 + 2] Addition (C5═C4)		
Acetyl VS1	AT	474.460	−183.033	−183.033	−196.249	−177.926	−177.893	−185.839
Diamino VS	AT	432.422	−136.303	−136.233	−148.188	−136.150	−136.142	−138.142
Acetoacetyl VS	HT	605.588	–	–	–	−315.860	−315.685	−332.551
Acetoacetyl VS	A/KT	605.588	–	–	–	−319.876	−319.869	−326.751
Mode (position)			Ene (C6═C1; H(N7))			[2 + 2] Addition (C1═C6)		
Acetoacetyl VS	HT	605.588	−328.207	−328.190	−365.427	−314.395	−314.394	−351.729
Mode (position)			Ene (C9═N8; H(N7))			[2 + 2] Addition (C9═N8)		
Acetoacetyl VS	HT	605.588	−328.209	−328.167	−355.021	−328.218	−328.044	−332.879
Acetoacetyl VS	A/KT	605.588	–	–	–	−319.249	−319.218	−332.879[b]
Mode (position)			Ene (C13═C14; H(N21))			[2 + 2] Addition (C13═C14)		
Yellow 3	AT	606.541	−151.798	−151.700	−177.463	−151.142	−151.135	−169.326
Acetyl VS2	AT	897.877	−317.225	−317.137	−345.632	−318.360	−318.342	−334.696
Ureido BF	AT	871.796	−363.927	−363.918	−395.860	−364.656	−364.645	−385.422
Pyridone BF	HT	721.672	–	–	–	−251.396	−251.374	−261.607
Pyridone BF	A/ET	721.672	–	–	–	−248.727	−248.677	−251.394
Mode (position)			Ene (C13═C14; H(Me))			[2 + 2] Addition (C13═C14)		
Methyl VS	AT	902.896	−252.377	−252.370	−279.328	−249.791	−249.697	−270.637

[a] Azo tautomer of dioxetanes was only made irrespective of the starting hydrazone tautomer.

[b] Hydrazone tautomer of dioxetanes was only made irrespective of the starting azo/keto tautomer.

than those mentioned above may also occur simultaneously. Thus, [2 + 2] addition may also generate the common product, as reported previously [1]. During exposure, this dye seemed to yield almost exclusively one kind of decomposed product and only a small amount of by-products. This may be consistent with the mechanisms explained above.

In order to examine the validity of the analyses mentioned throughout the text, and to determine whether a correlation between log k_0 and the $S^{(E)}_{m,n}$ values exists or not for the dyes examined, log k_0 was plotted on the ordinate using the experimental data. The plotting of the $S^{(E)}_{m,n}$ values on the abscissa required some selection: first, we introduced the double bond with highest reactivity, and then the other double bonds in decreasing order of contribution, one by one. It was observed that a better correlation with the common correlation line appeared if the value of $S^{(E)}_{m,n}(m,n:1,3{-}10,14)$ for Diamino VS was used together with the plots for all of the other dyes (cf. Fig. 5) than if the value of $S^{(E)}_{m,n}(m,n:1{-}10,14)$ was used. As mentioned below, the plots for the azobenzene dyes did not fit the plots for the pyrazolinylazo dyes and monoazo dyes from γ- and J-acids examined in previous studies [1,2].

3.5.1.2. *ATs of Acetyl VS1.*

This dye exists overwhelmingly as ATs in both the gas phase and water. The similarity between Diamino VS and Acetyl VS1 in d_{HOMO} and the smaller reactivity of this dye relative to the former may be noted from Table 2 and the results of photo-oxidative fading. The reactivities of the double bonds in the ATs of Acetyl VS1 may be estimated based on the values of $\Delta_f H^0$(gas) for the products (cf. Tables 7–9), as follows:

$$\begin{aligned}\mathrm{ene(C3{=}C4;H(N15)} &= [2+2]\mathrm{addition(C3{=}C2)}\\ &> [2+2]\mathrm{addition(C1{=}C6)}\\ &> \mathrm{ene(C1{=}C2;H(N15)}\\ &> [2+2]\mathrm{addition(C3{=}C4)}\\ &> \mathrm{ene(C5{=}C4;H(N16))}\\ &> [2+2]\mathrm{addition(C1{=}C2)}\\ &> [2+2]\mathrm{addition(C10{=}C9)}\\ &= [2+2]\mathrm{addition(C9{=}C14)}\\ &> [2+2]\mathrm{addition(C5{=}C4)}\\ &\gg [2+2]\mathrm{addition(N7{=}N8)}. \qquad (7)\end{aligned}$$

The order (7) was different from the order (6), while the orders for the two dyes based on the $S^{(E)}_{m,n}$ values were completely similar to each other except for the reactivity of the

Table 8
Heat of formation, $\Delta_f H^0$(gas) (kcal/mol), of intermediate and products in the ene and [2 + 2] cycloaddition reactions at the double bonds of C10=C9, C9=N8, C13=C14, C15=C16, C16=C17 and C15=C14 for A&HTs of azobenzene dyes with singlet oxygen

	Tautomer	M.W.	$\Delta_f H^0$(gas) of intermediate at TSG	$\Delta_f H^0$(gas) of intermediate	$\Delta_f H^0$(gas) of hydroperoxide	$\Delta_f H^0$(gas) of intermediate at TSG	$\Delta_f H^0$(gas) of intermediate	$\Delta_f H^0$(gas) of addition product
Mode (position)			Ene (C9=N8; H(N7))			[2 + 2] Addition (C9=N8)		
Acetoacetyl VS	HT	605.588	−328.209	−328.167	−355.021	−328.218	−328.044	−332.879
Mode (position)			Ene (C10=C9; H(N8))			[2 + 2] Addition (C10=C9)		
Acetyl VS1	AT	474.460	–	–	–	−175.913	−175.773	−192.797
Acetyl VS1	HT	474.460	–	–	–	−159.467	−159.462	−176.069
Diamino VS	AT	432.422	–	–	–	−136.037	−135.881	−152.383
Pyridone BF	HT	721.672	−253.189	−253.187	−292.754	−254.236	−254.232	−274.704
Mode (position)			Ene (C9=C10; H(Me))			[2 + 2] Addition (C9=C10)		
Acetoacetyl VS	A/KT	605.588	−321.109	−321.108	−360.630	−318.449	−318.408	−356.971
Mode (position)						[2 + 2] Addition (C12=C13)		
Acetyl VS1	HT	474.460	–	–	–	−159.460	−159.457	−165.392
Pyridone BF	HT	721.672	–	–	–	−255.246	−255.238	−273.879
Pyridone BF	A/ET	721.672	–	–	–	−249.138	−249.106	−269.874
Mode (position)			Ene (C3=C2; H(Me))			[2 + 2] Addition (C3=C2)		
Acetyl VS1	AT	474.460	–	–	–	−176.688	−176.605	−202.866
Diamino VS	AT	432.422	–	–	–	−136.076	−136.048	−158.768
Pyridone BF	HT	721.672	−255.359	−255.357	−299.516	−253.598	−253.596	−284.556
Pyridone BF	A/ET	721.672	−251.555	−251.554	−284.003	−251.537	−251.536	−270.697
Acetoacetyl VS	HT	605.588	–	–	–	−326.118	−326.093	−351.529
Acetoacetyl VS	A/KT	605.588	–	–	–	−319.303	−319.296	−344.651
Mode (position)			Ene (C3=C4; H(N16))			[2 + 2] Addition (C3=C4)		
Acetyl VS1	AT	474.460	−179.257	−179.248	−202.905[a]	−175.846	−175.844	−197.042
Diamino VS	AT	432.422	−135.563	−135.514	−164.903[a]	−135.072	−134.674	−159.979
Acetoacetyl VS	HT	605.588	–	–	–	−330.115	−330.107	−341.823
Acetoacetyl VS	A/KT	605.588	–	–	–	−319.612	−319.612	−334.175
Mode (position)			Ene (C3=C4; H(4′OH))			[2 + 2] Addition (C3=C4)		
Pyridone BF	A/ET	721.672	−248.684	−248.669	−297.005	−248.855	−248.852	−273.579

[a] Hydrazone tautomer of hydroperoxide was only made irrespective of the starting azo tautomer.

bond of N7=N8. As a whole, Diamino VS has a higher reactivity than Acetyl VS1.

The reactivity of the ATs at C2 may be excluded due to the very small value of d_{HOMO} at C2, while that at N7=N8 may be excluded due to the small value at N7 (0.006) in spite of the considerably high value of $f_r^{(E)}$. This dye has a lower reactivity than Diamino VS because of the difference in the reactivity at N7=N8. Although the reactivity of the double bond at C1=C2 for Acetyl VS1 was similar to that for Diamino VS, the reactivity at the double bonds of C3=C4 and C4=C5 for the Acetyl VS1 was found to be smaller than that for Diamino VS. (As in the case of Diamino VS, the values of $\Delta_f H^0$(gas) for the intermediates of Acetyl VS1 in PM5 geometry and in PM5 TSG (cf. Tables 7–9) gave different results.)

The reaction schemes for the reactions at these double bonds were identical to the corresponding reactions for Diamino VS. The absorption spectra of the decomposed products of this dye were also the same as those of Diamino VS within the experimental margin of error, although the two dyes were considerably different in the spectra of the original dyes and the rate of photo-oxidative fading (cf. Fig. 2). The similarity between the two dyes with regard to the spectra of the decomposed products may also corroborate the present discussion.

As in the case of Diamino VS, a good correlation between $\log k_0$ and the $S_{m,n}^{(E)}$ values for the ATs of this dye was found when the value of $S_{m,n}^{(E)}(m, n : 1, 3–6, 9, 10, 14)$, plotted against $\log k_0$, was used together with the plots of the other dyes, although the value was smaller than for Diamino VS.

3.5.2. Reaction modes of o-arylamino- or o-methyl-azobenzene dyes with triazinyl, and/or vinylsulfonyl, bridged by triazine ring, anchor

Four dyes, Yellow 3, Acetyl VS2, Ureido BF and Methyl VS, belong to this group and exist as ATs in both the gas phase and water (cf. Tables 2 and 3). The chemical structures of this group determined by naphthylamine → *o*-acylamino-substituted or *o*-methyl- benzene with a triazinylimino group as an MCT anchor or as a bridge group for a VS anchor (→ = diazotization and coupling). The d_{HOMO} for the ATs, listed in Tables 5 and 6, exhibited some common features with respect to distribution: the highest density was found at C13 (coupling site) and high densities were found at N19 and C16. This implies that photo-oxidation occurs predominantly at C13 and secondarily at C16. The $S_{m,n}^{(E)}$ values of the corresponding double bonds connected with these atoms may determine their reactivities. Large anchor groups with a triazine ring, however, suffer no strong

Table 9
Heat of formation, $\Delta_f H^0$(gas) (kcal/mol), of intermediates and products (1,2-dioxetane) in the [2 + 2] cycloaddition reactions at the possible double bonds of (C14═C15), (C14═C19), (C16═C17), (C17═C18), (C10═C11) and (C11═C12) for the predominant tautomer of dyes with $^1O_2$

	M.W.	$\Delta_f H^0$(gas) of intemediate at TSG	$\Delta_f H^0$(gas) of intermediate	$\Delta_f H^0$(gas) of hydroperoxide	$\Delta_f H^0$(gas) of intermediate at TSG	$\Delta_f H^0$(gas) of intermediate	$\Delta_f H^0$(gas) of addition product
Mode		[2 + 2] Addition (C1═C2) for HT			[2 + 2] Addition (C1═C6) for A/KT		
Acetoacetyl VS	605.588	−328.135	−328.116	−349.746	−319.275	−319.275	−340.458
Mode		[2 + 2] Addition (C9═C10) for A/KT			[2 + 2] Addition (C10═C11) for A/ET		
Pyridone BF	721.672	−248.869	−248.864	−267.928	−248.720	−248.662	−266.875
Acetoacetyl VS	605.588	−319.245	−319.177	−354.076	–	–	–
Mode		[2 + 2] Addition (C1═C6) for AT			[2 + 2] Addition (C9═C14) for A/ET		
Acetyl VS1	474.460	−176.340	−176.340	−199.374	–	–	–
Diamino VS	432.422	−135.728	−135.707	−159.067	–	–	–
Pyridone BF	721.672	–	–	–	−248.898	−248.868	−258.722
Mode		[2 + 2] Addition (C14═C15) for AT			[2 + 2] Addition (C15═C16) for AT		
Yellow 3	606.541	−151.776	−151.775	−172.684	−148.733	−148.689	−170.007
Acetyl VS2	897.877	−318.654	−318.654	−339.132	−316.735	−316.735	−332.838
Ureido BF	871.796	−361.828	−361.826	−383.212	−359.213	−359.171	−377.782
Methyl VS	902.896	−250.571	−250.543	−270.965	−248.051	−247.972	−267.904
Mode		[2 + 2] Addition (C16═C17) for AT			[2 + 2] Addition (C17═C18) for AT		
Yellow 3	606.541	−150.071	−150.059	−169.027	−148.659	−148.637	−171.416
Acetyl VS2	897.877	−319.476	−319.467	−340.686	−315.167	−315.167	−339.083
Ureido BF	871.796	−359.322	−359.257	−375.935	−361.880	−361.876	−382.802
Methyl VS	902.896	−248.421	−248.404	−270.516	−250.830	−250.813	−268.185
Mode		[2 + 2] Addition (C13═C18) for AT			[2 + 2] Addition (C1═10) for AT		
Yellow 3	606.541	−151.126	−151.123	−166.398	−148.814	−148.805	−174.580
Acetyl VS2	897.877	−316.308	−316.276	−337.819	−316.160	−316.158	−338.382
Ureido BF	871.796	−363.726	−363.725	−381.886	−361.781	−361.779	−387.864
Methyl VS	902.896	−250.656	−250.656	−270.063	−250.687	−250.491	−273.768
Mode		[2 + 2] Addition (C4═C9) for AT			[2 + 2] Addition (N11═N12) for AT		
Yellow 3	606.541	−148.771	−148.725	−162.792	−150.151	−150.009	−130.819
Acetyl VS2	897.877	−316.160	−316.152	−328.685	−316.386	−316.386	−300.310
Ureido BF	871.796	−361.781	−361.779	−359.155	−274.758	−274.758	−406.473
Methyl VS	902.896	−250.292	−250.285	−262.887	−186.941	−186.935	−255.046
Mode		[2 + 2] Addition (N7═N8) for AT			[2 + 2] Addition (N7═N8) for A/E(K)T		
Acetyl VS1	474.460	−176.587	−176.488	−159.638	–	–	–
Diamino VS	432.422	−136.052	−136.015	−119.066	–	–	–
Pyridone BF	721.672	–	–	–	−242.194	−242.185	−277.983
Acetoacetyl VS	605.588	–	–	–	−317.798	−317.793	−298.342

oxidative attack, while only small *o*-substituted phenyl rings do. Unfortunately, since large unsusceptible anchor groups may shield the phenyl group from any chemical change, as reflected in the absorption spectra of the decomposed products, it is difficult to analyze what reaction occurs in the phenyl rings except for the scission of the azo groups.

These four dyes have similar chemical structures resulting in low reactivities against $^1O_2$ or high lightfastness; three of the dyes in this group (Group C in Section 3.3) showed almost the same absorption spectra of the decomposed products in spite of the introduction of substituents in the triazine ring; the spectra were considerably different from those of Yellow 3, which has no phenyl group in the anchor.

3.5.2.1. Reaction modes for ATs of Yellow 3. This dye possesses an MCT anchor in the coupling component. The distribution of d_{HOMO} in Table 6 suggests the potential reactivities at the double bonds of C13═C14, C15═C16, C16═C17, C17═C18, C13═C18 and N11═N12. Because the d_{HOMO} at C15 may indicate the lower limit of reactivity, the reaction of C14═C15 against $^1O_2$ was also analyzed in order to confirm the contribution of C15 to the reactivity. The values of $\Delta_f H^0$(gas) for the reaction intermediates from the corresponding double bonds were nearly the same in PM5 TSG.

Based on an estimation of $\Delta_f H^0$(gas) for the products (cf. Tables 7–9), the order of the reactivities for the reaction modes was as follows:

$$\begin{aligned}\mathrm{ene}(\mathrm{C13{=}C14;H(N21)}) &\gg [2+2]\mathrm{addition}(\mathrm{C15{=}C14})\\ &> [2+2]\mathrm{addition}(\mathrm{C15{=}C16})\\ &> [2+2]\mathrm{addition}(\mathrm{C13{=}C14})\\ &\approx [2+2]\mathrm{addition}(\mathrm{C16{=}C17})\\ &> [2+2]\mathrm{addition}(\mathrm{C13{=}C18})\\ &> [2+2]\mathrm{addition}(\mathrm{C4{=}C9})\\ &\gg [2+2]\mathrm{addition}(\mathrm{N11{=}N12}).\end{aligned} \tag{8}$$

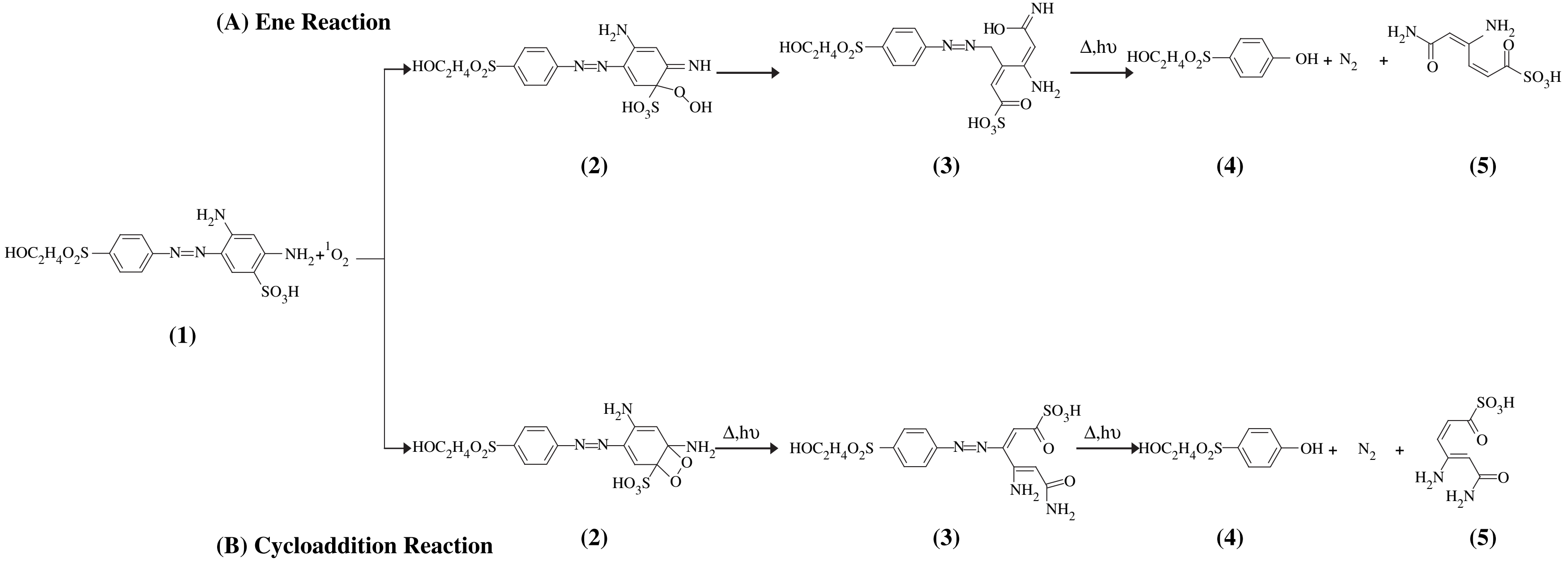

Scheme 1. (A) Ene (C5═C4; H(N16)) and (B) [2 + 2] cycloaddition (C5═C4) reactions of the ATs for Diamino VS and Acetyl VS1, which contain a vinylsulfonyl anchor in the coupling component, with singlet oxygen. In (A), (2): ene intermediate by the addition of singlet oxygen to the double bond at C5═C4, (3): the hydroperoxide via ene reaction, (4) and (5): thermal and/or photodecomposed products from the hydroperoxide via dediazotization, where some by-products other than (4) and (5) may be formed. In (B), (2): 1,2-dioxetane via [2 + 2] cycloaddition (C5═C4) (the intermediate by the parallel addition of $^1O_2$ to the double bond of N4═C5 was omitted), (3) thermal and/or photodecomposed products from the 1,2-dioxetanes, scission of C5═C4 bond, (4) and (5): thermal and/or photodecomposed products from (3) via dediazotization, where some by-products other than (4) and (5) may be formed. (see text.)

Along with the $S_{m,n}^{(E)}$ values (cf. Table 2) for several double bonds with potential reactivity in the HOMO of the coupling component and its almost vacancy in the diazo component (naphthalene ring) (cf. Table 6), the inequality (8) would indicate the same predominance of this mode as that based on the $S_{m,n}^{(E)}$ values, if ene (C13═C14; H(N21)) were chosen as the reaction site. The multiplicity factors to derive $f_r^{(E)}$ from d_{HOMO} at each atomic site were exceptionally large for this dye (cf. Section 3.5.2.5). Thus, the exclusion of reactivity was decided based on the values of $f_r^{(E)}$ and irrespective of the d_{HOMO} values. The reactivities of the double bonds of C13═C18, N11═N12, C14═C15, C15═C16 and C4═C9 for the ATs of Yellow 3 may be excluded due to the small values of d_{HOMO} at C18 (0.000), N12 (0.007), C15 (0.009) and C9 (0.003) (cf. Table 6). The results indicate that Yellow 3 possesses a relatively high resistance to oxidative attack.

The reaction scheme for ene (C13═C14; H (N21)) is illustrated in Scheme 2A, and that for [2 + 2] cycloaddition (C13═C14) in Scheme 2B. When only ene (C13═C14; H(N21)) occurred, a quinone-iminoquinone derivative bound with cellulose through an aminotriazinyl anchor could be observed in the absorption spectra of the decomposed products. If [2 + 2] cycloaddition (C13═C14) proceeded concurrently or exclusively, carbonyl fragments were formed accompanied by phenyl-ring opening, leading to a loss of aromaticity. Since [2 + 2] addition (C16═C17) may cause the bond scission of the imino bridge group, triazine residues could result. When [2 + 2] addition occurred at double bonds other than C13═C14, the ring opening at another sites could be observed, likewise with concurrent loss of aromaticity. As mentioned below, the absorption spectra of the decomposed products in the UV region, at wavelengths below 300 nm, showed clear double peaks, unlike the spectra of the other three dyes examined containing a triazinyl nucleus as the bridging group between the chromophore and the reactive anchor. This seems to indicate the occurrence of ene (C13═C14; H(N21)) for Yellow 3, but the concurrence of [2 + 2] addition (C16═C17) is open to debate. At the same time, the reactivity at the double bonds of N11═N12 and C4═C9 may be excluded due to the small value of d_{HOMO} at N12 (0.007) and C9 (0.003). In contrast to these double bonds, the reactivity at C1═C10 should be taken into consideration due to the large values of d_{HOMO} at C1(0.021) and C10 (0.026), in spite of the relatively small values of $f_r^{(E)}$. The reactivity at C18 may also be excluded due to the very small value of d_{HOMO} (0.000).

The plot of the value of $S_{m,n}^{(E)}(m, n : 1, 10, 13, 14, 16, 17)$ against $\log k_0$ gave a common correlation line with the plots of the other dyes examined. The addition of the contribution of the double bonds at N11═N12 or C15═C16 to this $S_{m,n}^{(E)}$ value resulted in a large deviation from the common line. As the $\Delta_f H^0$(gas) value indicates, this dye may exist as ATs in both the gas phase and water, and its reactivity is explained by the $f_r^{(E)}$ values only for the ATs.

3.5.2.2. Reaction modes for ATs of Ureido BF. Based on the values of $\Delta_f H^0$(gas) for the products resulting from reactions with $^1O_2$ (cf. Table 8), the reactivities of the modes can be ordered thus:

$$\begin{aligned}[2+2]\text{addition}(\text{N11}{=}\text{N12}) &> \text{ene}(\text{C13}{=}\text{C14};\text{H(N21)})\\ &\gg [2+2]\text{addition}(\text{C13}{=}\text{C14})\\ &\approx [2+2]\text{addition}(\text{C15}{=}\text{C14})\\ &> [2+2]\text{addition}(\text{C13}{=}\text{C18})\\ &> [2+2]\text{addition}(\text{C15}{=}\text{C16})\\ &> [2+2]\text{addition}(\text{C16}{=}\text{C17})\\ &\gg [2+2]\text{addition}(\text{C4}{=}\text{C9}).\end{aligned} \tag{9}$$

The values of $\Delta_f H^0$(gas) for the reaction intermediates stemming from these double bonds in PM5 TSG were nearly the same, as in the case of Yellow 3, except for the double bond of N11═N12. Since the value for N11═N12 was much higher (by ca. 90 kcal/mol) than the values for the other bonds, the reactivity of this bond may be excluded.

The estimation based on the $S_{m,n}^{(E)}$ value for each mode suggests that the [2 + 2] addition (C13═C14) has the highest reactivity and [2 + 2] cycloaddition (C16═C17) the second highest, followed by [2 + 2] addition (N11═N12) (cf. Table 3). The reaction schemes for some of the modes are shown in Scheme 2A and B, although the chemical structures must be read as those of Ureido BF. But the central part around the reaction site may be the same as that of Yellow 3.

Comparably to the case of Yellow 3, the reactivity of C1═C10, C15═16 and C17═C18 may be excluded due to the small value of d_{HOMO} at C1 (0.006), C15 (0.005) and C18 (0.000). As in the case of Yellow 3, the contribution of the double bonds of N11═N12 and C4═C9 may be excluded due to the small value of d_{HOMO} at N12 (0.008) and C9 (0.000). These results are summarized in Table 4; they indicate that this dye has the lowest number of reactive sites, confined to the sites common to all of the dyes of this group. Thus, the reaction schemes of various modes for the dyes in this group may be essentially the same, as shown in Table 4. Unfortunately, the details pertaining to each dye cannot be discussed due to the resemblance of the spectra of their decomposed products.

As in the case of Yellow 3, the plot of $S_{m,n}^{(E)}$ $(m, n : 13, 14, 16, 17)$ for Ureido BF against $\log k_0$, together with the plots of the other dyes examined, gave a common correlation line. This is applicable to the other two dyes as well, as explained below.

3.5.2.3. Reaction modes for ATs of Methyl VS. The estimation of the reactivity for each mode for this dye based on the $\Delta_f H^0$(gas) values of the corresponding reaction products listed

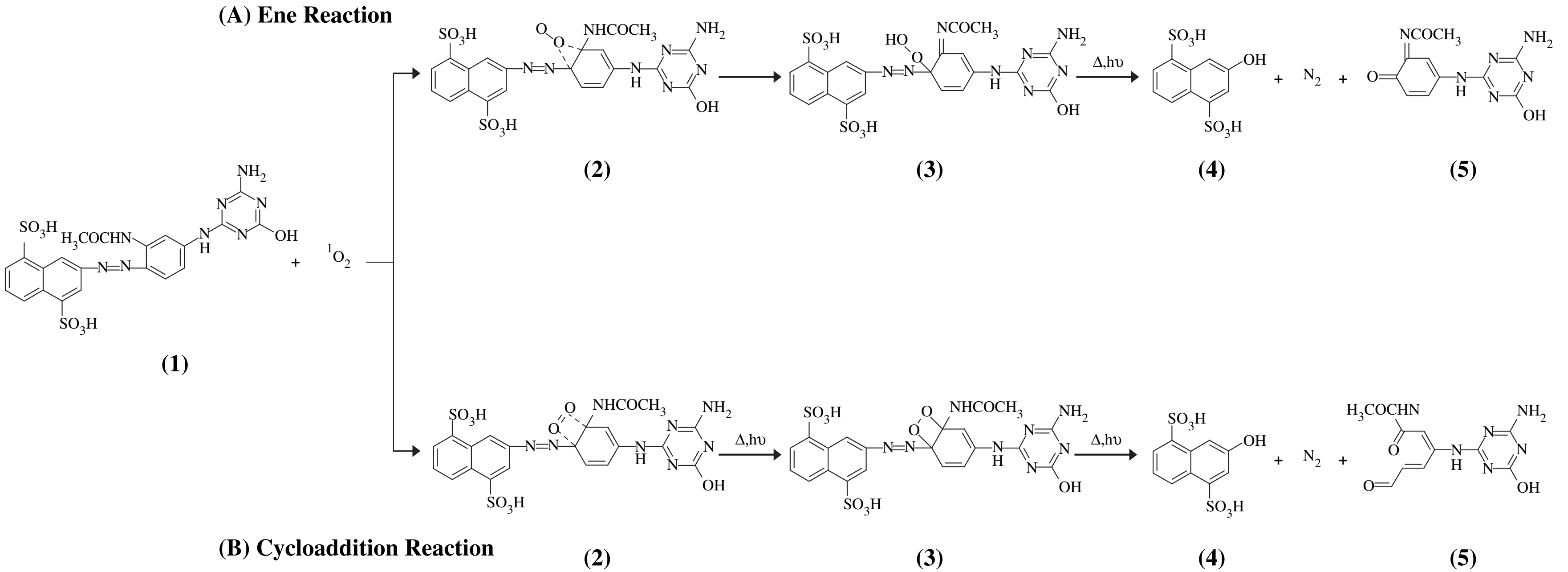

Scheme 2. (A) Ene (C13═C14; H(N21)) and (B) [2 + 2] cycloaddition (C13═C14) reactions of the ATs for group C dyes, which contain a vinylsulfonyl anchor in the coupling component, with singlet oxygen. In (A), (2): ene intermediate by the addition of singlet oxygen to the double bond at C13═C14, (3): the hydroperoxide via ene reaction, (4) and (5): thermal and/or photodecomposed products from the hydroperoxide via dediazotization, where some by-products other than (4) and (5) may be formed. In (B), (2): 1,2-dioxetane via [2 + 2] cycloaddition (N4═C5) (the intermediate by the parallel addition of $^1O_2$ to the double bond of N4═C5 was omitted), (3) thermal and/or photodecomposed products from the 1,2-dioxetanes, scission of N4═C5 bond, (4) and (5): thermal and/or photodecomposed products from (3) via dediazotization, where some by-products other than (4) and (5) may be formed. (see text.)

in Tables 7–9 gave an order of reactivity almost similar to that for Yellow 3 and Ureido BF, as follows:

$$\begin{aligned}\text{ene}(\text{C13}{=}\text{C14};\text{H(Me)}) &> [2+2]\text{addition}(\text{C1}{=}\text{C10})\\ &> [2+2]\text{addition}(\text{C15}{=}\text{C14})\\ &\approx [2+2]\text{addition}(\text{C13}{=}\text{C14})\\ &\approx [2+2]\text{addition}(\text{C16}{=}\text{C17})\\ &\approx [2+2]\text{addition}(\text{C13}{=}\text{C18})\\ &> [2+2]\text{addition}(\text{C17}{=}\text{C18})\\ &> [2+2]\text{addition}(\text{C15}{=}\text{C16})\\ &> [2+2]\text{addition}(\text{C4}{=}\text{C9})\\ &> [2+2]\text{addition}(\text{N11}{=}\text{N12}).\end{aligned} \tag{10}$$

This estimation was consistent with the estimation based on the values of $\Delta_f H^0$(gas) for the products: it reflects the order of magnitudes of $\Delta_f H^0$(gas) and $S^{(E)}_{m,n}$. The values of $\Delta_f H^0$(gas) for the reaction intermediates in PM5 TSG were around 250 kcal/mol for all of the reaction modes, with the exception of the value for N11=N12, which was more than 60 kcal/mol higher than the other values, and the values of $\Delta_f H^0$(gas) for the product was even higher (cf. Table 9). This may be a property which this dye has in common with Yellow 3. This may mean that [2 + 2] addition (N11=N12) stops before the intermediate stage in spite of the fair reactivity toward $^1O_2$. As a result, the reactivity at N11=N12 may be excluded. The reactivity at C1=C2 may also be excluded due to the lower-limit value of $f_r^{(E)}$ (0.025) at C2.

The correlation between $\log k_0$ and the $S^{(E)}_{m,n}(m,n:13{-}18)$ values for this dye was also consistent with that of all of the other dyes examined, although some deviation in the direction of lower reactivity was observed. Thus, Scheme 2A and B may also be applied to this dye. The absorption spectra of decomposed products can be interpreted as being self-consistent, since the absorption spectra of these three dyes seemed to possess the same pattern, as mentioned above.

3.5.2.4. Reaction modes for ATs of Acetyl VS2. Like in the case of the other three dyes of this group mentioned above, the reactivity for each mode was estimated based on the values of $\Delta_f H^0$(gas) for the products reacting with $^1O_2$, and the order of reactivity was as follows:

$$\begin{aligned}\text{ene}(\text{C13}{=}\text{C14};\text{H(N21)}) &> [2+2]\text{addition}(\text{C16}{=}\text{C17})\\ &> [2+2]\text{addition}(\text{C15}{=}\text{C14})\\ &= [2+2]\text{addition}(\text{C17}{=}\text{C18})\\ &> [2+2]\text{addition}(\text{C1}{=}\text{C10})\\ &\approx [2+2]\text{addition}(\text{C13}{=}\text{C18})\\ &> [2+2]\text{addition}(\text{C13}{=}\text{C14})\\ &> [2+2]\text{addition}(\text{C15}{=}\text{C16})\\ &> [2+2]\text{addition}(\text{C4}{=}\text{C9})\\ &> [2+2]\text{addition}(\text{N11}{=}\text{N12}).\end{aligned} \tag{11}$$

The order of reactivity based on $S^{(E)}_{m,n}$ is different from the order (11). The d_{HOMO} was concentrated almost exclusively at the central phenyl ring and at the bridging groups of N11=N12 and N19, while the d_{HOMO} values were extremely low at the naphthalene ring (cf. Table 6). The $\Delta_f H^0$(gas) value for the intermediates from N11=N12 was almost the same as those from the other double bonds mentioned above. The reactivity at the double bond of C1=C10 may be excluded due to the small value of d_{HOMO} at C10 (0.004). As shown in Table 4, the high reactivity of the phenyl group and its bridging group may be a distinctive characteristic of the dyes of this group.

The plot of $S^{(E)}_{m,n}(m,n:11{-}18)$ against $\log k_0$ showed a good coincidence with the common correlation line for all the dyes examined, with a slight deviation in the direction of lower reactivity.

The absorption spectra of the decomposed products for this dye were very similar in pattern to those of two other dyes in this group. Unfortunately, the details cannot be discussed due to the resemblance of the spectra of their decomposed products, as in the case of the other dyes in this group.

3.5.2.5. An analysis on the effect of triazinyl group on the reactivity of dyes. When the reactivities of the four dyes in Group C were compared with those of Group A, the former were found to be markedly lower than the latter. Whether the discrepancy is attributable to the substitution of the triazine ring or not will be discussed semi-quantitatively, from the viewpoint of the MO theory. Since these dyes are too large for an analysis of the MO to be carried out in further detail due to the great number of occupied orbitals (cf. Table 10), an analysis was conducted by separating the MO parameters into their constituents, as shown in Table 10. Six of the eight dyes possessed nearly the same sum of d_{HOMO} for the coupling component, and that of Yellow 3 was rather small while that of Methyl VS was still smaller. The sum of $f_r^{(E)}$ for each constituent is also listed in parentheses in Table 10. The distribution of the sum of d_{HOMO} and $f_r^{(E)}$ to other parts of the molecule varies with the dyes; the diazo components, azo groups, imino bridge groups and triazine groups contain various values of d_{HOMO} and $f_r^{(E)}$. The d_{HOMO} of the triazine ring has no reactivity due to the electron distribution to alternate atoms, one of the processes by which reactivity is lowered. The electrons at the bridge groups also show no reactivity due to a lack of double bonds. The diazo component may possess values of d_{HOMO} and $f_r^{(E)}$ peculiar to its structure; these values may be little affected by the triazine ring, which is located at a large distance.

In spite of the variations in the reactivity of these constituents, however, the center of reactivity is located in the coupling components. The sum of $f_r^{(E)}$ representing the reactivity of Group A was considerably larger than that of Group C, indicating the difference in reactivity, irrespective of the similar values of the sums of d_{HOMO}. Since the difference in structure between groups A and C lies in the triazine ring, the decrease in the reactivity of the coupling component must be due to the ring. The triazine ring has little effect on the values of d_{HOMO}, but a strong one on those of $f_r^{(E)}$. The electrons in orbitals lower than HOMO clearly contribute to the reactivity, although those in HOMO already show a similar reactivity. Thus, the differences in reactivity between groups A and C may be attributed to the triazine

Table 10
Sum of electron density in each part of the whole molecule and sum of $f_r^{(E)}$ in the part[a] (cf. Tables 5 and 6)

Dye	No. of occupied MO	Diazo component	Azo group	Coupling component	Bridge group	Triazine ring	Amino or imino bridge group	Summation $S_{m,n}^{(E)}(S_{m,n}^{(E)})$
		C1–C10	N11–N12	C13–C18	N19	C20–N25	N26–	
Yellow 3	101	0.088 (0.090)	0.078 (0.0)	0.501 (0.757)	0.131 (0.0)	0.076 (0.0)	0.112 (0.0)	0.986 (0.847)
Acetyl VS2	151	0.032 (0.0)	0.074 (0.105)	0.535 (0.731)	0.214 (0.0)	0.126 (0.0)	0.001 (0.0)	0.981 (0.836)
Ureido BF	145	0.057 (0.0)	0.094 (0.0)	0.530 (0.723)	0.115 (0.0)	0.066 (0.0)	0.130 (0.0)	0.992 (0.723)
Methyl VS	151	0.166 (0.115)	0.126 (0.0)	0.484 (0.669)	0.131 (0.0)	0.077 (0.0)	0.003[b] (0.0)	0.984 (0.784)
		C9–C14	N7–N8	C1–C6	N16		N15	
Diamino VS	70	0.168 (0.188)	0.126 (0.244)	0.535 (0.971)	0.114 (0.0)		0.041 (0.0)	0.984 (1.403)
Acetyl VS1	78	0.089 (0.180)	0.154 (0.0)	0.559 (0.970)	0.200 (0.0)		0.000 (0.0)	1.002 (1.150)

The total of d_{HOMO} is normalized to be 1.0 [31].

[a] Sum of $f_r^{(E)}$ at the site which contributes to the reactivity is described in parentheses.

[b] d_{HOMO} at carbon atom of *o*-methyl group.

ring, which affects the distribution of electrons in orbitals lower rather than in HOMO.

The differences in reactivity among dyes of Group C, on the other hand, seem to be due to the shift of d_{HOMO} from the coupling component to other parts, although the electrons in the other parts of some dyes also exhibit reactivities peculiar to the components at which they exist. The electrons in HOMO in the coupling component of Methyl VS, which had the lowest reactivity, shifted the reactivity to almost all of the other components, most of which had exhibited no reactivity, and had displayed the smallest d_{HOMO} sum in the group. The small value resulted in a lower reactivity. However, the electrons at the diazo component exhibiting some reactivity may raise the dye's reactivity, resulting in a reactivity similar to that of Ureido BF. On the contrary, in spite of the higher reactivity in the coupling component of Ureido BF as compared to that of Methyl VS, Ureido BF has a reactivity similar to Methyl VS due to the lack of reactivity of the electrons in the other parts. The differences in reactivity at the coupling component can also be examined in the foregoing sections.

3.5.3. Reaction modes of phenylazopyridone dye

The photochemical reactions of pyridone, including the reactions with $^1O_2$, have been extensively studied [35–37]. Pyridoneazo dyes have typical yellow chromophores with intermediate lightfastness. Since pyrazolinylazo dyes contain three carbonyl groups which enable them to exhibit keto–enol tautomerism in addition to AHT, they possess several tautomers as a result of their combination with an azo group and three keto and/or enol groups. The chemical structures with higher stability in the gas phase and water were as follows:

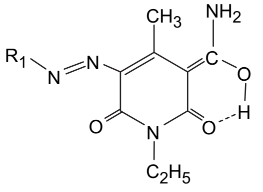

AT

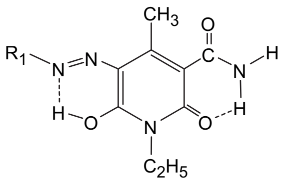

A/ET

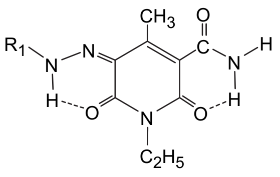

HT

where R_1 denotes the residue of the diazo component with a reactive anchor. The whole structure is shown in Section 2.1. The values of their Δ_fH^0 are listed in Table 3, which also shows that the predominant tautomers in the gas phase are overwhelmingly HTs and those in water a mixture of A/ETs and HTs (population ratio ≈ 1.0). As with the dyes mentioned above, the reactivities of the HTs and A/ETs are analyzed next.

3.5.3.1. HTs of Pyridone BF.

Due to the fixed double bonds in pyridone ring and active hydrogen for ene reaction, this dye possesses strong possibility to suffer ene and [2 + 2] cycloaddition reactions as summarized in Table 4. Although the position of double bonds may depend on the AHT of this dye, since the addition of $^1O_2$ may occur to any positions other than the fixed sites by changing the tautomerism, positions other than the fixed double bonds may have some reactivity toward $^1O_2$. However, because the reactivity of each tautomer is individually analyzed, no change of tautomerism during the addition of $^1O_2$ is taken into consideration.

The double bonds with potential reactivity are C1=N7, C3=C2, C9=C10, C12=C13, and C13=C14 from d_{HOMO} in Table 5. The d_{HOMO} existed only at C2=C3 in the pyridone ring and hydrazone azo group, and concentrated in the phenyl ring of diazo component. From the values of Δ_fH^0(gas) for the reaction products calculated (cf. Tables 7 and 8), the order of reactivity of each mode was estimated as follows:

$$\begin{aligned}\mathrm{ene}(\mathrm{C1{=}N7};\mathrm{H(N8)}) &\approx \mathrm{ene}(\mathrm{C3{=}C2};\mathrm{H(Me)})\\ &> \mathrm{ene}(\mathrm{C10{=}C9};\mathrm{H(N8)})\\ &> [2+2]\mathrm{addition}(\mathrm{C3{=}C2})\\ &> [2+2]\mathrm{addition}(\mathrm{C10{=}C9})\\ &> [2+2]\mathrm{addition}(\mathrm{C12{=}C13})\\ &> [2+2]\mathrm{addition}(\mathrm{C1{=}N7})\\ &> [2+2]\mathrm{addition}(\mathrm{C13{=}C14}). \qquad (12)\end{aligned}$$

They are similar to the estimation by $S^{(E)}_{m,n}$ values (cf. Table 3). Although there are few values of d_{HOMO} at N5 (0.000) and C6 (0.000), the positions may not contribute the reactivity due to their small values. The values of $\Delta_f H^0(\mathrm{gas})$ for the intermediates at the PM5 TSG from all the reaction modes of the corresponding double bonds were nearly the same as each other. No ene (C10=C9; H(N8)) was exceptional.

No reaction schemes for all the eight modes are drawn, because they may be easily analogized with the schemes shown already. Ene and [2 + 2] cycloaddition reactions at C1=N7 resulted in the scission of the double bond to cause dediazoniation. Although all reaction schemes for the possible modes are not illustrated, the other modes of reaction may perform ring opening of pyridone ring as a result of the formation of hydroperoxides (via ene reaction) and of dioxetanes (via [2 + 2] addition). The ring opening may generate unstable oxidized compounds with carbonyl fragments, which may suffer thermal and/or photodecomposition accompanied with dediazoniation. A phenol derivative bound with cellulose through large anchor system may be formed. The UV spectra of large double peaks may prove this fact (cf. Fig. 4), the generation of one kind of decomposed product.

Plotting the value of $S^{(E)}_{m,n}(m,n:1,7;2,3;9,10;12{-}14)$ for the HTs of Pyridone BF against $\log k_0$ together with their values of the other dyes examined showed a considerable deviation sidewise from the common correlation line in the smaller direction, as shown in Fig. 5.

3.5.3.2. A/ETs of Pyridone BF. The values of d_{HOMO} listed in Table 5 show that the double bonds of C1=C2, C1=C6, C2=C3, N7=N8, C9=C10, C9=C14, C10=C11, C12=C13 and C13=C14 are possibly reactive, while C1=C6, C3=C4, C4=N5 and C10=C11 may be excluded due to the very small values of d_{HOMO} at C4 (0.006), N5 (0.001), C6 (0.008) and C11 (0.000). Besides the reactive sites of the HTs, only the N8 site added to the contribution of the A/ETs. But the magnitudes of d_{HOMO} or $f_r^{(E)}$ for the A/ETs were as a whole larger than those for the HTs. This explains why A/ETs show higher reactivities than HTs.

Based on the calculated values of $\Delta_f H^0(\mathrm{gas})$ for the reaction products (cf. Tables 7 and 8) and excluding the double bonds mentioned above, the order of reactivity for the modes was estimated as follows:

$$\begin{aligned}\mathrm{ene}(\mathrm{C1{=}C2};\mathrm{H(Me)}) &> [2+2]\mathrm{addition}(\mathrm{N7{=}N8})\\ &> [2+2]\mathrm{addition}(\mathrm{C1{=}C2})\\ &> [2+2]\mathrm{addition}(\mathrm{C2{=}C3})\\ &> [2+2]\mathrm{addition}(\mathrm{C9{=}C10})\\ &\approx [2+2]\mathrm{addition}(\mathrm{C12{=}C13})\\ &\approx [2+2]\mathrm{addition}(\mathrm{C10{=}C11})\\ &> [2+2]\mathrm{addition}(\mathrm{C9{=}C14})\\ &> [2+2]\mathrm{addition}(\mathrm{C13{=}C14}). \qquad (13)\end{aligned}$$

The values of $\Delta_f H^0(\mathrm{gas})$ for the intermediate in PM5 TSG for each mode were similar. Since, like in the other cases, the $S^{(E)}_{m,n}$ values for these modes, listed in Table 3, may describe the sum of the reactivity for each mode, the values of $S^{(E)}_{m,n}(m,n:1{-}3,7{-}10,12{-}14)$ were plotted against $\log k_0$. The plot showed a small deviation in the direction of higher reactivity. When the value of $S^{(E)}_{m,n}(m,n:1{-}3,7{-}10,12{-}14)$ for the A/ETs and that of $S^{(E)}_{m,n}(m,n:1{-}3,7,9,10,12{-}14)$ for the HTs were plotted against $\log k_0$, the segment connecting both points intersected the common correlation line, as shown in Fig. 5. If this dye existed as a mixture of HTs and A/ETs on cellulose, the $S^{(E)}_{m,n}$ values would predict the observed values for the reactions with $^1O_2$. Unfortunately, however, this line of investigation cannot be pursued further, because the populations of HTs and A/KTs on cellulose cannot be determined. Another way to explain the reactivity of this dye must be found.

The absorption spectra of the decomposed products showed the existence of triazine and phenyl rings. Since the spectra from these reaction modes might be different from each other in the third phenyl ring, there might be no contradiction between the spectra and the MO theory. Therefore, the details of the reaction mechanisms could not be determined based on the analyses of the spectra.

In reality, since the AHT of this dye on cellulose may be more complex, the reaction schemes cannot be discussed based on the absorption spectra of the decomposed products.

3.5.4. Reaction modes of Acetoacetyl VS

A yellow azoic coupling component was developed as the yellow chromophore of this reactive dye. As shown in Table 3, this dye may exist exclusively as HTs in water, but in the gas phase A/KTs may predominate in a mixture with HTs. The chemical structures of the tautomers are as follows (the substituents on the phenyl ring are omitted):

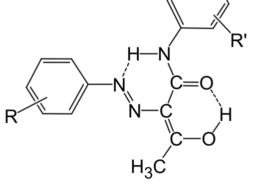

A/KTs

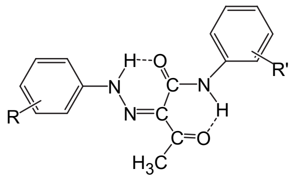

HTs

3.5.4.1. HTs. The d_{HOMO}, listed in Table 5, is concentrated at the phenyl ring of the diazo component and at the azo group. Since the d_{HOMO} values are large for the phenyl ring, this dye may possess a high reactivity. Based on the distribution of d_{HOMO}, the double bonds with high reactivities are summarized as modes of reaction in Table 3. Based on the values of $\Delta_f H^0$(gas) for the reaction products (cf. Tables 7 and 8), the order of reactivity for these modes is estimated as follows:

$$\begin{aligned}\mathrm{ene(C6{=}C1;H(N7))} &> \mathrm{ene(C9{=}N8;H(N7))}\\ &> [2+2]\mathrm{addition(C6{=}C1)}\\ &\approx [2+2]\mathrm{addition(C2{=}C3)}\\ &> [2+2]\mathrm{addition(C1{=}C2)}\\ &> [2+2]\mathrm{addition(C3{=}C4)}\\ &> [2+2]\mathrm{addition(C9{=}N8)}\\ &\approx [2+2]\mathrm{addition(C5{=}C4)}. \qquad (14)\end{aligned}$$

The reactivity of the double bond of C2=C3 may be excluded due to the very small value of d_{HOMO} (0.007) at C2. The values of $\Delta_f H^0$(gas) for the reaction intermediate in PM5 TSG were not different from each other. The magnitudes of the $S^{(E)}_{m,n}$ values for the six double bonds were as follows:

$$\begin{aligned}\mathrm{C6{=}C1} &> \mathrm{C3{=}C4} > \mathrm{C4{=}C5} > \mathrm{C2{=}C3}\\ &> \mathrm{C1{=}C2} \gg \mathrm{C9{=}N8}. \qquad (15)\end{aligned}$$

The inequalities (14) and (15) are different. Since d_{HOMO} at N8 was very small (0.008), the reactivity of the double bond of C9=N8 may be excluded. The plot of the value of $S^{(E)}_{m,n}(m,n : 6,1; 2,3; 4,5)$ against $\log k_0$, together with the values for the other dyes examined, showed a considerable deviation in the direction of lower reactivity from the common correlation line, as shown Fig. 5.

Although the schemes are not given, ene (C9=N8; H(N7)) and ene (C6=C1; H(N7)) as well as the [2 + 2] additions may be interpreted in analogy to the ene and [2 + 2] addition reactions explained above. The two ene reactions may proceed concurrently with [2 + 2] addition (C6=C1, C3=C4, and C4=C5). Although no schemes for the modes are given, it can be assumed that several modes in inequality (15) may generate a phenol derivative bound with cellulose through a VS anchor as the main product, while the other modes may result in the ring opening of phenyl, but the residue may be bound with cellulose through the VS anchor. If only the phenol derivative bound with cellulose were the decomposed product, the absorption spectra would be identical with those for Yellow 17 reported previously [1]. Some similarities were indeed found between the spectra, although these were not completely identical. This may prove the validity of the present schemes indirectly, although some vagueness remains.

3.5.4.2. A/KTs. Based on the values of $\Delta_f H^0$(gas) for the products of the reaction with $^1O_2$ (cf. Table 7), the reactivities of the modes might be ordered thus:

$$\begin{aligned}\mathrm{ene(C9{=}C10;H(Me))} &> [2+2]\mathrm{addition(C9{=}C10)}\\ &\gg [2+2]\mathrm{addition(C2{=}C3)}\\ &> [2+2]\mathrm{addition(C6{=}C1)}\\ &> [2+2]\mathrm{addition(C3{=}C4)}\\ &> [2+2]\mathrm{addition(C9{=}N8)}\\ &> [2+2]\mathrm{addition(C4{=}C5)}\\ &> [2+2]\mathrm{addition(N7{=}N8)}. \qquad (16)\end{aligned}$$

Since the results of the MO calculation indicated the double bond character of C9=N8 and C9=C10 for the A/KTs, the reactivity of the bonds was taken into consideration. It is possible that [2 + 2] addition (C9=N8) resulted in the production of HTs. The inequality (16) shows that [2 + 2] addition (C9=C10) and ene (C9=C10; H(Me)) are the most probable modes. Ene (C9=N8; H(N7)) is not possible due to the lack of H(N7). The value of $\Delta_f H^0$(gas) in PM5 TSG for the reaction intermediates from these double bonds were nearly the same. Based on the $S^{(E)}_{m,n}$ values, the order of reactivity for the double bonds was found to be the following:

$$\begin{aligned}\mathrm{C1{=}C6} \approx \mathrm{C9{=}N8} \approx \mathrm{C9{=}C10} &> \mathrm{C2{=}C3} > \mathrm{C3{=}C4}\\ &> \mathrm{C4{=}C5} > \mathrm{N7{=}N8}. \qquad (17)\end{aligned}$$

The two relations do not coincide. As in the case of the other dyes, the plot of the $S^{(E)}_{m,n}(m,n : 1{-}10)$ value against $\log k_0$ showed a fair coincidence with the common correlation line, with only a small deviation in the direction of higher reactivity (Fig. 5). If the contribution of both tautomers to the reactivity were taken into consideration, the reactivity estimated by the MO theory would perhaps coincide with the common correlation line of $S^{(E)}_{m,n}$ plotted against $\log k_0$, but the ratio between the tautomer populations cannot be determined.

Since, as in the case of the HTs, the reaction modes occurred at the sites bound with azo groups, the decomposed products from the A/KTs were similar to each other. The absorption spectra shown in Fig. 2c resembled that of Yellow 17 in pattern [1]. This may indicate the validity of the main schemes, but the differences in the schemes cannot be deduced based on the differences in the spectra.

4. Summary

Based on the present and the previous papers [1], the reactivities of yellow reactive dyes, such as pyrazolinylazo dyes and azobenzenes, toward $^1O_2$ were analyzed in terms of the frontier orbital theory. The results can be summarized as an analysis of the relationship between the reactivity and the chemical structure of reactive azo dyes, as follows:

1. Applying the same analytical procedure to the photooxidation of a series of azobenzene dyes, the same conclusion was derived by extending the validity of the procedure.
2. The reactivity, as described by the $S^{(E)}_{m,n}$ value (the sum of $f^{(E)}_r$ at the probable double bonds) defined by Eq. (5), showed a close correlation between $S^{(E)}_{m,n}$ and $\log k_0$ for a series of reactive dyes.
3. The $S^{(E)}_{m,n}$ value described the total reactivity of a dye toward $^1O_2$. Each element, $f^{(E)}_r$, of $S^{(E)}_{m,n}$ shows what sites

possess reactivity (cf. Table 4) and the extent of each reactivity (cf. Tables 2 and 3).

4. Analyses in terms of $f_r^{(E)}$ also clarified the conditions of non-reactivity for particular sites.
5. The shifting of electrons to non-reactive sites is the key to inducing low reactivity in the dye, although d_{HOMO} must be estimated based on the MO theory.
6. Introducing substituents that shift the electrons from a particular site of high reactivity does not always result in a lowering of the total reactivity.
7. Applying PM5 analysis to reactive dyes or aromatics may result in the molecular design of dyes with low reactivity toward $^1O_2$. This is a QSPR in the reactivity analysis for aromatics.
8. The superimposition of the correlation line of $S_{m,n}^{(E)}$ vs. $\log k_0$ for pyrazolinylazo dyes on that for azobenzene dyes resulted in two parallel lines with the same slope.
9. The two lines may converge into a common correlation line, if the modification of the HOMO–LUMO interaction through the use of the orbital energy differences is precise, although this was impossible with the present software. The present estimation of E_{LUMO} for $^1O_2$ seemed to contain errors too large for it to coincide with the correlation lines for different series of dyes.
10. The triazinyl rings in the dyes of Group C have the effect of lowering the electron density on the MO in the coupling component to values lower than those in HOMO, in spite of having no effect on d_{HOMO}, resulting in dyes with low reactivity toward $^1O_2$.
11. Depending upon the tautomers, the reactivities of the azo dyes against $^1O_2$, as estimated by the frontier orbital theory, were different from each other. Among the azobenzene dyes examined, the HTs were found to possess lower reactivities against $^1O_2$ than ATs. The HTs of the two series of dyes examined achieved the key conditions (cf. item 4 above) for low reactivity.
12. Moreover, it may be impossible in principle for azo dyes with low molecular weights but with high lightfastness to give high color values. Dyes with low molecular weights should possess high reactivity.

Acknowledgement

This work was supported by a Grant-in-Aid for Scientific Research given by the Ministry of Education, Culture, Sports, Science and Technology, Japan.

References

[1] Hihara T, Okada Y, Morita Z. Photo-oxidation of pyrazolinylazo dyes and an analysis of their reactivity as azo and hydrazone tautomers using the semiempirical molecular orbital PM5 method. Dyes and Pigments 2006;69(2):151–76.

[2] Hihara T, Okada Y, Morita Z. A semiempirical molecular orbital study on the photo-reactivity of monoazo reactive dyes derived from γ- and J-acids. Dyes and Pigments 2007;73(2):141–61.

[3] Albini A, Fagnoni M. Oxidation of aromatics. In: Horspool WM, Lenci F, editors. CRC handbook of organic photochemistry and photobiology. 2nd ed. Boca Raton: CRC Press; 2003. p. 45-1–45-19 [chapter 45].

[4] Brauer H-D, Schmidt R. Cycloaddition reactions involving $4n+2$ electrons. Photochromism based on the reversible reaction of singlet oxygen with aromatic compounds. In: Dürr H, Bouas-Laurent H, editors. Photochromism: molecules and systems. Studies in organic chemistry, vol. 40. Amsterdam: Elsevier; 1990. p. 631–53 [chapter 15].

[5] Yoshioka Y, Yamanaka S, Yamada S, Kawakami T, Nishino M, Yamaguchi K, et al. Theoretical and experimental studies of a charge-transfer mechanism for biomimetic oxygenations of phenol and indole derivatives. Bulletin of the Chemical Society of Japan 1996;69:2701–22.

[6] Liwo A, Dyl D, Jeziorek D, Nowacka M, Ossowski T, Woźnicki W. MCSCF study of singlet oxygen addition to ethanol – a model of photooxidation reactions of unsaturated and aromatic compounds bearing hydroxy groups. Journal of Computational Chemistry 1997;18(13):1668–81.

[7] Gollnick K, Griesbeck A. Singlet oxygen photooxygenation of furans. Isolation and reactions of $[4+2]$-cycloaddition products. Tetrahedron 1985;41(11):2057–68.

[8] Skew C, Kang P, Khan S, Foote CS. Low-temperature photosensitized oxidation of a guanosine derivative. Journal of the American Chemical Society 2002;124(15):3905–13.

[9] Adam W, Andler S, Ballmaier D, Emmert S, Epe B, Grimm G, et al. Oxidative DNA damage induced by dioxetanes, photosensitizing ketones and photo-Fenton reagents. Recent Results in Cancer Research 1997;143(Risk and progression factors in carcinogenesis):21–34.

[10] Murgida DH, Aramendía PF, Balsells RE. Photosensitized oxidation of oxopurines by Rose Bengal. Photochemistry and Photobiology 1998;68(4):467–73.

[11] Adam W, Saha-Möller CR, Schönberger A. Type I and type II photosensitized oxidative modifications of 2′-deoxyguanosine by triplet-excited ketones generated thermally from the 1,2-dioxatane HTMD. Journal of the American Chemical Society 1997;119(4):719–23.

[12] Hihara T, Okada Y, Morita Z. An analysis of azo–hydrazone tautomerism of reactive azobenzene and pyrazolinylazo dyes, using semiempirical molecular orbital PM5 method. Dyes and Pigments 2004;61(3):199–225.

[13] Hihara T, Okada Y, Morita Z. Azo–hydrazone tautomerism of phenylazonaphthol sulfonates and their analysis using semiempirical molecular orbital PM5 method. Dyes and Pigments 2003;59(1):25–41.

[14] Hihara T, Okada Y, Morita Z. Reactivity of phenylazonaphthol sulfonates, their estimation by semiempirical molecular orbital PM5 method, and the relation between their reactivity and azo–hydrazone tautomerism. Dyes and Pigments 2003;59(3):201–22.

[15] Okada Y, Hirose M, Kato T, Motomura H, Morita Z. Photofading of vinylsulfonyl reactive dyes on cellulose under wet conditions. Dyes and Pigments 1990;14:113–27.

[16] Hihara T, Okada Y, Morita Z. Relationship between photochemical properties and colourfastness due to light-related effects concerning monoazo reactive dyes derived from H-acid, γ-acid, and related naphthalene sulfonic acids. Dyes and Pigments 2004;60(1):23–48.

[17] Lambert CR, Kochevar IE. Does Rose Bengal generate superoxide anion? Journal of the American Chemical Society 1996;118(13):3297–8.

[18] Bonnett R. Chemical aspects of photodynamic therapy. Amsterdam: Gordon and Breach Science Publishers; 2000.

[19] Okada Y, Kato T, Motomura H, Morita Z. Fading mechanism of reactive dyes on cellulose by simultaneous effects of light and perspiration. Sen'i Gakkaishi 1990;46(8):346–55.

[20] Okada Y, Morita Z. Fading of some vinylsulfonyl reactive dyes on cellulose under various conditions. Dyes and Pigments 1992;18(4):259–70.

[21] Okada Y, Sato E, Motomura H, Morita Z. Photofading of monochlorotriazinyl reactive dyes on cellulose under wet conditions. Dyes and Pigments 1992;19(1):1–19.

[22] Okada Y, Orikasa K, Motomura H, Morita Z. Oxidative and reductive fading of monochlorotriazinyl reactive dyes on cellulose under wet conditions. Dyes and Pigments 1992;19(3):203–14.

[23] Okada Y, Fukuoka F, Morita Z. Environmental effects of oxygen on the fading of monochlorotriazinyl reactive dyes on cotton fabrics. Dyes and Pigments 1998;37(1):47–64.

[24] Morita Z, Hada S. A semiempirical molecular orbital study on the reaction of an aminopyrazolinyl azo dye with singlet molecular oxygen. Dyes and Pigments 1999;41(1):1–10.

[25] Frimer AA, Stephenson LM. The singlet oxygen ene reaction. In: Frimer AA, editor. Singlet O2. Reaction modes and products, part 1, vol. II. Boca Raton: CRC Press; 1985. p. 68–91 [chapter 3].

[26] Yamaguchi K. Theoretical calculations of singlet oxygen reactions. In: Frimer AA, editor. Singlet O2. Reaction modes and products, part 2, vol. III. Boca Raton: CRC Press; 1985. p. 119–251 [chapter 2].

[27] Orfanopoulos M. Singlet oxygen ene-sensitizer photo-oxygenations: Stereochemistry and mechanism. Molecular and Supramolecular Photochemistry 2001;8:243–85.

[28] Griesbeck AG, El-Idreesy TT, Adam W, Krebs O. Ene-reactions with singlet oxygen. In: Horspool WM, Lenci F, editors. CRC handbook of organic photochemistry and photobiology. 2nd ed., vol. 8. Boca Raton: CRC Press; 2003. p. 1–20 [chapter 8].

[29] Adam W, Beinhauer A, Hauer H. Activation parameters and excitation yields of 1,2-dioxetane chemiluminescence. In: Scaiano JC, editor. Handbook of organic photochemistry, vol. 2. Boca Raton: CRC Press; 1989. p. 271–327 [chapter 12].

[30] Fukui K, Fujimoto H. Frontier orbitals and reaction paths. Singapore: World Scientific; 1997.

[31] Fukui K, Yonezawa T, Shingu H. A molecular orbital theory of reactivity in aromatic hydrocarbons. Journal of Chemical Physics 1952;20(4):722–5.

[32] Fukui K, Yonezawa T, Nagata C, Shingu H. Molecular orbital theory of orientation in aromatic, heteroaromatic and other conjugated molecules. Journal of Chemical Physics 1954;22(8):1433–42.

[33] Fukui K, Yonezawa T, Nagata C. Interrelations of quantum–mechanical quantities concerning chemical reactivity of conjugated molecules. Journal of Chemical Physics 1957;26(4):831–41.

[34] CAChe Reference Guide. CAChe Reference Guide 4.9; 3-9–3-10. Fujitsu Ltd.

[35] Sato E, Ikeda Y, Kanaoka Y. Photosensitized oxygenation of 2-pyridones. Heterocycles 1987;25:65–8.

[36] Sieburth SMcN. Photochemical reactivity of pyridones. In: Horspool WM, Lenci F, editors. CRC handbook of organic photochemistry and photobiology. 2nd ed. Boca Raton: CRC Press; 2003. p. 103-1–103-18 [chapter 103].

[37] Bouas-Laurent H, Desvergne J-P. Cycloaddition reactions involving 4*n* electrons: $(4+4)$ cycloaddition reactions between unsaturated conjugated systems. In: Dürr H, Bouas-Laurent H, editors. Studies in organic chemistry. Photochromism: molecules and systems, vol. 40. Amsterdam: Elsevier; 1990. p. 561–630 [chapter 14].